JOURNAL OF THE Electrochemical Society

VOLUME 95 NUMBER 5

November 1949

Published by
THE ELECTROCHEMICAL SOCIETY

Journal of The Electrochemical Society

Number 5 November 1949 Volume 96

Current Affairs

Editorial: A Rose By Any Other Name ... 197
News Notes ... 198
Meetings and Divisions ... 198
Personals ... 199
New Members ... 200
Book Reviews ... 201
Contributing Structures ... 202
Letters to the Editor ... 203
Future Meetings ... 204
Recent Patents ... 204

Technical Notes

Some Considerations on the Physics of Wooden Membranes ... 205

Technical Papers

Influence of Temperature on Efficiencies of Zinc Sulfide Phosphors Containing Silver and Cadmium ... 207
Some New Copper-Activated Phosphors Containing Cadmium, Manganese, and Beryllium ... 227
Luminescence and Conduction in Solid Solutions of Certain Sulfides in Transition Salts ... 237
Some Solid Solutions of the Rare Earth Sulfides in Strontium Sulfide ... 261
Effect of Mineral Admixtures, Electrolytes, and Rate of Precipitation of Aluminum in Basic Aluminum Sulfate ... 269
Paper Plate Electrodes for Respiratory Measurements ... 279

R. T. Ubbig
Editor

F. L. LaQue
Business Manager

E. J. Read
Technical Editor

Review Staff
I. M. Bialosky
Paul S. Bradley
N. C. Cahoon
C. L. Faust
H. C. Froelich
A. F. Pavlica
E. B. Saubestre
Sherlock Swann, Jr.
Arthur J. Weith

Eleanor Held
Managing Editor

H. C. Oxford
Associate Editor

U. B. Thomas
Associate Editor

R. M. Burns
Consultant

THE INFLUENCE OF TEMPERATURE ON THE EFFICIENCIES OF ZINC SULFIDE PHOSPHORS CONTAINING SILVER AND COBALT[1]

C. G. A. HILL AND H. A. KLASENS

Material Research Laboratory, Philips Electrical Limited, Surrey, England

ABSTRACT

The temperature dependence of the blue fluorescence of zinc sulfide phosphors containing 10^{-2} per cent silver and $0–10^{-3}$ per cent cobalt, under λ 3650 excitation, has been measured over the temperature range of 120–600 K. The form of the temperature dependence curve and its shift toward lower temperatures on the introduction of cobalt are interpreted in terms of the theory of hole migration. The activation energy for hole migration from silver luminescence centers is found to be $0.36 \pm .02$ electron volts. An estimate of the number of intrinsic killer centers in terms of cobalt centers is obtained.

INTRODUCTION

Various theoretical explanations of the temperature dependence of fluorescence in crystal phosphors have been advanced, but owing to the paucity of reliable measurements, there has been little attempt to examine these theories quantitatively. Recent theoretical studies by Klasens *et al.* (1, 2) related the fluorescence efficiency of the phosphor to the temperature, the intensity of excitation, and the nature and number of impurity centers. The intensity dependence has been measured at a few fixed temperatures (3, 7, 8). It was clear that a more detailed study of the temperature changes was needed, and this paper gives the results of such measurements.

EXPERIMENTAL

Phosphors.—Unless otherwise stated, the phosphors used were prepared in these laboratories using the following standard procedure.

Pure zinc sulfide, obtained by precipitation with hydrogen sulfide from an acid solution of a zinc salt, was mixed with a solution of the activating compounds together with 2 per cent by weight of sodium chloride (relative to the amount of ZnS). The mixture was dried at 110 C and the powder transferred to a silica crucible in which it was fired for 30 minutes at 850 C in an atmosphere of nitrogen. At the conclusion of the firing, the furnace power was cut off and the temperature allowed to fall to 400 C before the crucible was removed. The phosphors were then washed with distilled water until the wash water showed only a trace of chloride ions.

The resulting powders consist of cubic ZnS crystals having an average particle size of 2 μ.

In these experiments, a silver concentration of 10^{-2} per cent by weight

[1]Manuscript received February 7, 1949. This paper prepared for delivery before the Philadelphia Meeting, May 4 to 7, 1949.

(= $9 \cdot 10^{-5}$ atoms Ag per atom Zn) was used throughout. Analysis of the fired phosphors showed that the differences between the nominal and actual concentration of Ag and Co were insignificant.

Measurements.—The apparatus with which the temperature dependence of the fluorescence was measured is sketched in Fig. 1. The phosphor was spread in a thin layer on the recessed surface of the aluminum block, A. This was cooled by immersing the protruding copper cylinder, B, in liquid nitrogen. When the temperature indicated by the copper-constantan thermocouple at C was sufficiently low, the liquid nitrogen was removed and a pair of electric heaters of the type used for heating small mercury diffusion pumps was clipped onto the copper cylinder, and the current was switched on. Readings were taken continuously during the warming

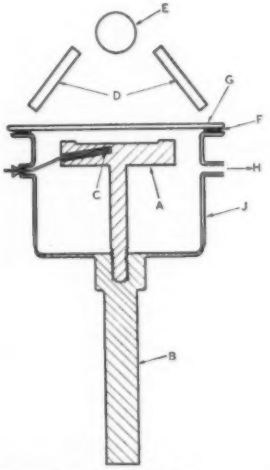

FIG. 1. Sketch of a vertical section through the apparatus used for measuring the temperature dependence of fluorescence efficiency.

of the phosphor. Two barrier layer photocells, D, were used to measure the intensity of the luminescence. Filters were used to isolate the required parts of the spectrum. For the blue band emitted by silver activated phosphors, a Wratten 47 was used, while ultraviolet reflected from the phosphor and its surroundings was prevented from reaching the photocell by a Chromex 2324 filter which is practically nonfluorescent. The green band emitted by some phosphors was isolated by 2 mm thickness of Chance OY2 glass, together with the Chromex 2324. A small proportion of the green band is transmitted by the Wratten 47 filter, and corrections were made for this when necessary. The exciting source, E, was a 125 watt MBW mercury arc in a nickel oxide glass envelope. During measurements, the lamp current was manually adjusted to a constant value by means of a variable transformer. The photocells could be connected alternately to a low resistance galvanometer via a shunt box, and the

combination gave a linear relation between light intensity and galvanometer reading within 1 per cent over the intensity range encountered.

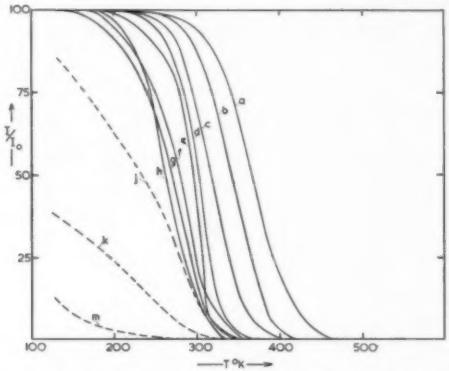

FIG. 2. Temperature dependence curves of ZnS phosphors activated with 10^{-2} per cent silver and containing various amounts of cobalt. The letters refer to Table I.

TABLE I

Phosphor number	Curve Fig. 2	Cobalt concentration: Wt % × 10^{2}	Cobalt concentration: Co atoms / Ag atoms × 100	killer centers / lumin. centers × 100	$T_{\frac{1}{2}}$ (K)	Remarks
154/7	a	0		0.3	372	
179/3		0.1	0.018	0.32	366	
179/4		0.5	0.092	0.39	366	
179/2		1.0	0.18	0.48	365	
179/1	b	5.0	0.92	1.2	342	
174/2	c	10	1.84	2.1	318	
178/1		20	3.7	4.0	315	fired in air
178/8		20	3.7	4.0	315	
179/8	d	20	3.7	4.0	302	
174/4		30	5.5	5.8	294	
178/3	e	40	7.4	7.7	286	quenched
178/9		40	7.4	7.7	290	
174/6	f	60	11.1	11.4	282	
174/7	g	70	12.6	12.9	271	
174/5	j	80	14.9	15.2	—	
178/6	h	80	14.9	15.2	268	fired at 960 C
174/8	k	100	18.4	18.7	—	
174/9	m	200	36.8	37.1	—	

RESULTS

Fig. 2 shows the temperature dependences of the blue emission band (λ max 4550 Å) for a few members of a series of phosphors containing increasing amounts of cobalt, and in Table I data concerning the complete series are listed. Where possible, the maxima of all curves have been put equal to 100. The column headed $T_{\frac{1}{2}}$ in Table I records the temperature

at which the ordinates of the curves pass through the value 50. No detailed measurements of the absolute efficiencies of these phosphors at their optimum temperatures have been made, but these did not differ by more than ±5 per cent. The fall in efficiency at low temperatures found by many workers is, in our opinion, probably due to contamination

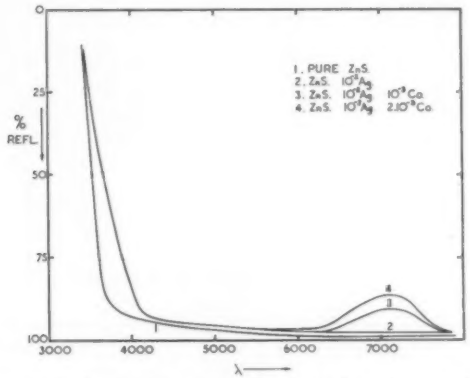

FIG. 3. Reflection spectra of ZnS containing silver and cobalt

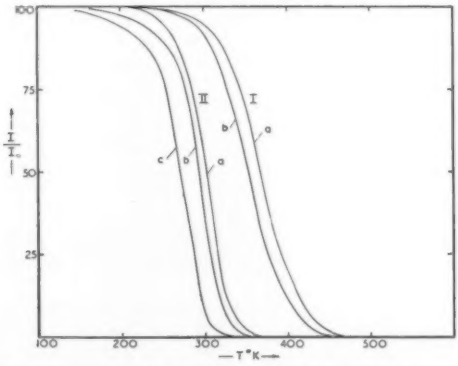

FIG. 4. The effect of varying the exciting intensity on the temperature dependence of two ZnS: Ag phosphors. I. No cobalt, (*a*) exciting intensity 1.0; (*b*) exciting intensity 0.22. II. $2 \cdot 10^{-4}$ per cent Co, (*a*) exciting intensity 1.0; (*b*) exciting intensity 0.22; (*c*) exciting intensity 0.03.

with iron, and can be reduced to negligible proportions by suitable purification of the raw materials. Conversely, addition of iron to ZnS:Ag phosphors can so reduce the efficiency at low temperatures that the phosphor may only fluoresce appreciably over a narrow temperature range.

The introduction of cobalt had no influence on the spectral distribution of the blue band and no new emission attributable to the cobalt could be

found in the wavelength range 3700–9000 Å. An absorption occurring at about 7000 Å was found in the phosphors having high cobalt concentrations as shown in Fig. 3.

The influence of the exciting intensity on the temperature dependence is shown in Fig. 4 for a phosphor containing silver only, and also for one containing both silver and cobalt.

DISCUSSION

Form of the temperature dependence curve.—It has been suggested (4), (5), (6) that the fall in luminescence efficiency of crystal phosphors with increasing temperature is due to the thermal excitation of electrons in the excited levels of the luminescent centers to a point at which the potential energies of the excited and ground states are close to one another. At this point, electrons can return to the ground state without emitting radiation. Such a mechanism would result in a temperature dependence curve of the form

$$I_t = \frac{I_0}{1 + Se^{-E/kT}}. \tag{I}$$

Since the quenching is solely a function of the energy levels of the center itself, the temperature of quenching should be independent of the exciting intensity, and can only be influenced by the presence of other impurities if the latter are near neighbors of the luminescence centers in the lattice.

That such an expression is inadequate in our case is shown by the shift in quenching temperature with changes in exciting intensity (Fig. 4). Also the effect of quantities of cobalt very much smaller than the number of silver atoms present is too great to allow of explanation by the suggestion of spatial association. These facts all indicate that the mechanism of temperature quenching is more complex.

Klasens (1) has attributed the effect of exciting intensity and cobalt concentration to hole-migration. This theory has been worked out in more detail by Wise and Klasens (2).[2]

With one kind of luminescent center and one kind of killer center, we have under equilibrium conditions:[3]

$$n = n_1 + n_2 + n_f \tag{II}$$

$$\frac{dn_1}{dt} = \mu_1 J - \beta_1 n n_1 - \gamma_{1f} n_1 + \Gamma_{f1} n_f = 0 \tag{III}$$

$$\frac{dn_2}{dt} = \mu_2 J - \beta_2 n n_2 - \gamma_{2f} n_2 + \Gamma_{f2} n_f = 0 \tag{IV}$$

$$(\mu_1 + \mu_2) J = n(\beta_1 n_1 + \beta_2 n_2) \tag{V}$$

n = concentration of free electrons.
n_1 = concentration of holes in luminescent centers.

[2] A similar treatment, details of which were not available at the time of writing, has been developed by M. Schön, *Z. Physik*, **119**, 463 (1942); *Ann. Physik*, **3**, 22 (1948).

[3] It is assumed that there is no saturation of the fluorescence, i.e., that n_1 is always small compared with the total number of centers.

n_f = concentration of holes in the filled band.
n_2 = concentration of holes in killer centers.
μ_1 (μ_2) = absorption coefficient in luminescent (killer) centers.
$\gamma_{1f}\, n_1$, ($\gamma_{2f}\, n_2$) = rate of escape of holes from luminescent (killer) centers.
$\gamma_t l$ = rate of release of electrons from traps.
J = exciting intensity.
I = fluorescence intensity.
I_0 = maximum fluorescence intensity on the temperature dependence curve.
$\gamma_{1f} = Se^{-E/kt}$
$\beta_1\, nn_1$, ($\beta_2\, nn_2$) = rate of recombination between electrons and holes in luminescent centers (killers).
$\Gamma_{f1}\, n_f = \alpha_1\, n_f\, (N_1 - n_1)$ = rate of recombination between free holes and luminescent centers (N_1).

If $\mu_2 \ll \mu_1$ and the escape of holes from killer centers can be neglected it follows from (III), (IV), and (V) that

$$n_1 = \frac{\mu_1 J}{\beta_1 n + \dfrac{\gamma_{1f} \cdot \Gamma_{f2}}{\Gamma_{f1} + \Gamma_{f2}}}, \qquad I = \beta_1 n n_1 = \frac{\mu_1 J}{1 + \dfrac{\gamma_{1f} \cdot \Gamma_{f2}}{\beta_1 n(\Gamma_{f1} + \Gamma_{f2})}} \tag{VI}$$

The effect of the intensity on the efficiency of zinc sulfide phosphors containing silver and cobalt as found by Klasens, Ramsden, and Chow Quantie (3) has been explained (2) by assuming that the rate of recombination of electrons with holes at killing centers is much faster than that of electrons with ionized silver centers ($\beta_2 \gg \beta_1$). This means that the number of holes in killing centers will always be small compared with the number of holes in luminescent centers over a large temperature range and we can write by approximation (n_f and $n_2 \ll n_1$ and thus $n_1 \backsim n$)

$$I = \beta_1 n^2, \qquad n = \left(\frac{I}{\beta_1}\right)^{1/2}$$

Equation (VI) then becomes

$$\frac{\mu_1 J}{I} = 1 + \frac{\gamma_{1f} \cdot \Gamma_{f2}}{(\beta_1 I)^{1/2}(\Gamma_{f1} + \Gamma_{f2})}. \tag{VII}$$

For $T = 0$, $\mu_1 J = I_0$

and
$$\left(\frac{I_0}{I}\right)^{1/2} - \left(\frac{I}{I_0}\right)^{1/2} = Be^{-E/kT} \tag{VIII}$$

where
$$B = \frac{S \cdot \Gamma_{f2}}{(I_0 \beta_1)^{1/2}(\Gamma_{f1} + \Gamma_{f2})}$$

B is approximately proportional to the number of killer centers and independent of temperature. We have, therefore,

$$\ln \left\{ \left(\frac{I_0}{I}\right)^{1/2} - \left(\frac{I}{I_0}\right)^{1/2} \right\} = \ln B - E/kT$$

Using this expression and plotting against $1/T$, the curves in Fig. 5 were obtained for phosphors containing small amounts of cobalt ($<3\cdot10^{-4}$ % Co). They consist mainly of parallel straight lines, the slope of which gives $E = 0.36 \pm 0.02$ electron volts (ev). This is in agreement with the value of 0.37 ev found by Klasens, Ramsden, and Chow Quantie (3). Deviations from the parallel lines were found at low temperatures for phosphors with high cobalt concentrations. However, for most curves, it was still possible to estimate the value of I_0. These deviations are of great interest in themselves and they will now be considered.

The form of the temperature dependence curve at high cobalt concentrations. —As the cobalt concentration is increased, there is a regular shift in the temperature dependence curve toward lower temperatures until the cobalt concentration reaches about $3\cdot10^{-4}$ per cent. Above this concentration,

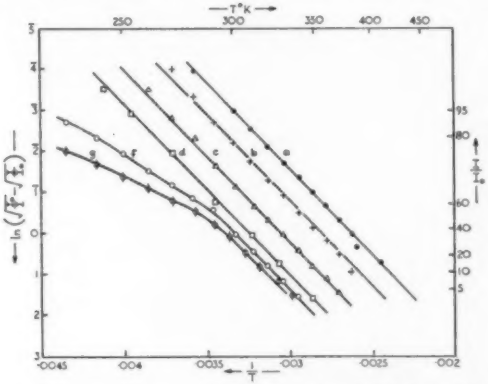

FIG. 5. Some of the curves of Fig. 2 replotted as $\ln\left\{\left(\frac{I_0}{I}\right)^{\frac{1}{2}} - \left(\frac{I}{I_0}\right)^{\frac{1}{2}}\right\}$ against $1/T$.

changes occur in the form of the temperature dependence curve which becomes progressively more marked as the concentration is increased.

The extent of this change in shape is strongly influenced by changes in the preparative conditions of the phosphor. This effect is clearly evident in Fig. 2 by comparison of curves h and j corresponding to two phosphors of the same, high, cobalt concentration fired at 800 C and 950 C, respectively. For the lower cobalt concentrations this sensitivity was not found, phosphors being easily reproducible in all respects.

At first sight, the change in slope which occurs with increasing cobalt concentration implies a change in the value of E. However, this quantity, which is the activation energy for hole migration from the blue emitting centers, should only be very slightly affected by the amounts of cobalt present in these phosphors. Furthermore, any lowering of the value of E due to the presence of cobalt would be expected to be accompanied by a shift of the blue emission band toward shorter wavelengths. No such shift was observed. One is, therefore, led to seek some other factor which may influence the temperature dependence.

Examination of the curves of Fig. 2 and 5 shows that the change in character occurs at roughly the same temperature in all cases. This suggests that the reason for the change is not primarily connected with the presence of the cobalt, but comes into play when the temperature dependence curve has been shifted to a low enough temperature. If this is the case, shifting the curve by other means should have a similar result. This can be done by lowering the exciting intensity and, for a phosphor having an intermediate cobalt concentration, the expected result was obtained. The curves are plotted in Fig. 6. At high exciting intensities a linear plot is obtained, but at low intensities part of the curve deviates in the same way as for phosphors with higher cobalt concentrations.

It is suggested that electron traps which are filled at low temperatures, and which are known to be present in these phosphors, are responsible

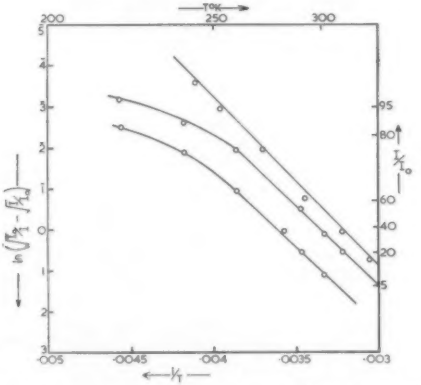

FIG. 6. Curves IIa, b, c of Fig. 4 replotted as $\ln\left\{\left(\frac{I_0}{I}\right)^{\frac{1}{2}} - \left(\frac{I}{I_0}\right)^{\frac{1}{2}}\right\}$ against $1/T$.

for the deviations. Their effect on the equilibrium between free electrons, holes, and centers has been discussed briefly by Wise and Klasens (2).

With l trapped electrons and L-l empty traps (not associated with ionized centers) we have

$$\frac{dl}{dt} = \alpha n(L - l) - \gamma_t l = 0$$

$$l = \frac{\alpha L n}{\alpha n + \gamma_t} \tag{IX}$$

$$I = \beta_1 n n_1 = \beta_1 n^2 \left(1 + \frac{\alpha L}{\alpha n + \gamma_t}\right)$$

$$n = \left(\frac{I}{\beta_1}\right)^{1/2} \cdot \frac{1}{\left(1 + \frac{\alpha L}{\alpha n + \gamma_t}\right)^{1/2}}$$

Substituting in (VI) gives

$$\frac{\mu_1 J}{I} = 1 + \frac{\gamma_{1f} \cdot \Gamma_{f2}}{(\beta_1 I)^{1/2} \cdot (\Gamma_{f2} + \Gamma_{f1})} \cdot \left(1 + \frac{\alpha L}{\alpha n + \gamma_t}\right)^{1/2}$$

or

$$\ln \left\{ \left(\frac{I_0}{I}\right)^{1/2} - \left(\frac{I}{I_0}\right)^{1/2} \right\} = -\frac{E}{kT} + F_t + \ln B \qquad \text{(XI)}$$

where

$$F_t = \ln \left(1 + \frac{\alpha L}{\alpha n + \gamma_t}\right)^{1/2} \qquad \text{(XII)}$$

At high temperatures γ_t, which is of the form $s_t e^{-E/kT}$ with E equal

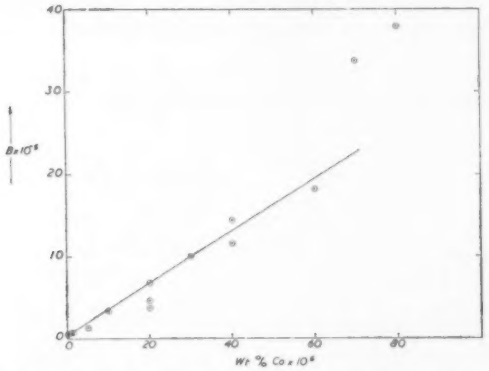

FIG. 7. The relation between the cobalt concentration and B of equation (VIII).

to the trap depth, becomes very large and the effect of the traps is negligible. At low temperature

$$\ln \left\{ \left(\frac{I_0}{I}\right)^{1/2} - \left(\frac{I}{I_0}\right)^{1/2} \right\}$$

becomes too large by a factor F_t. This factor is not only dependent on temperature but also on the ratio of $L:n$ and can only become significant if L is at least of the same order of magnitude as n, or larger. In other words, the phosphor must contain a large number of shallow traps. It is quite possible that the depth and the number of these traps is directly influenced by the higher cobalt concentrations. If the cobalt centers act as shallow traps when not ionized, a possible explanation for the very short lifetime of positive holes at cobalt centers would be that as soon as a hole is captured by a cobalt center it recombines with the electron already trapped there.

The value of F_t has been calculated for the curves of Fig. 6 (II) and for some other phosphors. The accuracy of the measurements is not sufficient

to allow verification of equation (XI) but it is found that when F_t is large it does vary linearly with $1/T$. For the curves of Fig. 6 (II), the trap depth obtained from this calculation is 0.5 ev and the corresponding value of the factor $\frac{\alpha_t L}{S_t}$ for the escape of electrons from these traps is 6×10^{10}.

The influence of the cobalt concentration—other killer centers.—The value of the factor B in equation (VIII) was calculated for most of the phosphors from the values of $T_{\frac{1}{2}}$, taking for E the average value of 0.36 ev. In Fig. 7, B is plotted against the concentration of cobalt. When the latter is less than $70 \cdot 10^{-5}$ per cent, the results can be represented by a straight line, but for higher concentrations the B is too high, owing to the distortion of the temperature dependence curves discussed above, by the factor F_t. It will be noticed that B is still finite for phosphors to which no cobalt has been added, indicating that other killing centers are present in addition. This is, of course, not unexpected, but by plotting the results in this way we find that we can estimate the number of these centers in terms of cobalt centers.

If we put $\Gamma_{f3} = \alpha_3 N_3$, where N_3 is the number of intrinsic killing centers and α_3 their cross section for hole capture, we have

$$B = \frac{S}{(I_0\beta_1)^{1/2}} \cdot \frac{\Gamma_{f2} + \Gamma_{f3}}{\Gamma_{f1} + \Gamma_{f2} + \Gamma_{f3}} \tag{XIII}$$

and

$$B_0 = \frac{S}{(I_0\beta_1)^{1/2}} \cdot \frac{\Gamma_{f3}}{\Gamma_{f1} + \Gamma_{f3}} \tag{XIV}$$

when there is no cobalt present.

Since B appears to vary linearly with Γ_{f2} $(= \alpha_2 N_2)$, we can expand (XIII) as far as the term in Γ_{f2}^2, thus

$$B = \frac{1}{\Gamma_{f1} + \Gamma_{f3}} \cdot \frac{S}{(I_0\beta_1)^{1/2}} \left[\Gamma_{f3} + \frac{\Gamma_{f2}\Gamma_{f1}}{\Gamma_{f1} + \Gamma_{f3}} \left\{ 1 - \frac{\Gamma_{f2}}{\Gamma_{f1} + \Gamma_{f3}} \right\} \right] \tag{XV}$$

Estimating that the true value of B in Fig. 7 does not deviate by more than 10 per cent from the straight line at 40×10^{-5} per cent Co we can say that in (XV)

$$\frac{\Gamma_{f2}}{\Gamma_{f1} + \Gamma_{f3}} < 0.1 \tag{XVI}$$

Dividing the slope of the line by B_0 we have

$$\frac{\alpha_2 \Gamma_{f1}}{\Gamma_{f3}(\Gamma_{f1} + \Gamma_{f3})} = 6.3 \cdot 10^4 \tag{XVII}$$

Dividing (XVI) by (XVII), it follows that $\Gamma_{f3}/\Gamma_{f1} < 0.004$ and so from (XVII) we can say $\alpha_2/\alpha_3 N_3 = 6.3 \cdot 10^4$. Assuming that $\alpha_2 = \alpha_3$ we find that the concentration of intrinsic killing centers is equivalent to a cobalt concentration of $1.6 \cdot 10^{-5}$ weight per cent. In column 5 of Table I, this equivalent number of intrinsic killing centers has been added to the number of cobalt centers.

The presence of the intrinsic killing centers can be explained in various ways. It is possible that the starting material already contains enough impurities to cause this effect. On the other hand, it is conceivable that the structure defects present in most crystal lattices act as killing centers. To investigate this further, a well-crystallized commercial zinc sulfide phosphor activated with silver was crushed in a mortar. The phosphor became grey in appearance and an additional absorption extending over the whole range of the visible spectrum was found. The value of $T_{\frac{1}{2}}$ had decreased from 378 to 342 K. This shift is probably partly caused by a reduction of the exciting intensity. That the number of killing centers had increased was, however, proved conclusively by a measurement of

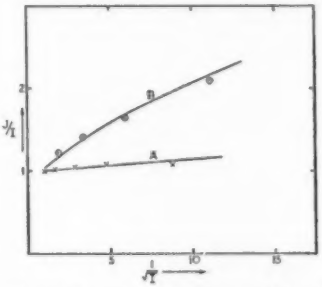

FIG. 8. The intensity dependence of a well-crystallized ZnS: Ag phosphor (A) before, and (B) after, milling. For each curve, I has been put = 1 for $J = 1$.

the intensity dependence, the results of which are shown in Fig. 8. The slope of the curve J/I against $\left(\frac{1}{I}\right)^{\frac{1}{2}}$ has increased after milling in accordance with an increase of the value of Γ_{f_2} in equation (VII).

CONCLUSIONS

1. It has been shown that the form of the temperature dependence curve for zinc sulfide phosphors containing silver as an activator and cobalt as a killer cannot be explained satisfactorily by a simple quenching process within the luminescent center, but that for low cobalt concentrations a satisfactory agreement between theory and experiment can be obtained using the theory of hole migration. The experimental value of the activation energy involved in this process agrees with that obtained from measurements of the intensity dependence of fluorescence.

2. At high cobalt concentrations deviations from the theoretical curves occur which are shown to be not primarily due to the presence of the cobalt, but to be a secondary consequence of the large shift of the temperature dependence curve toward lower temperatures caused by the cobalt. Similar deviations are obtained by the use of very low exciting intensities with phosphors containing lower cobalt concentrations. It is suggested that these deviations are caused by the presence of electron traps.

3. The influence of the cobalt concentration on the quenching temperature of the phosphor is in accordance with the theory of hole migration. The effective number of intrinsic killer centers present has been measured in terms of the cobalt concentration. It is shown that the presence of lattice defects can account for the presence of these killer centers.

ACKNOWLEDGMENTS

Acknowledgments are due to Dr. S. Rothschild for the preparation of the phosphors, and to Mr. M. E. Wise for invaluable theoretical discussions. We wish to thank Mr. J. A. M. van Moll and the directors of Philips Electrical Ltd. for permission to publish this paper.

Any discussion of this paper will appear in the discussion section of Volume 96 of the TRANSACTIONS of the Society.

REFERENCES

1. H. A. KLASENS, *Nature*, **158**, 306 (1946).
2. M. E. WISE AND H. A. KLASENS, *J. Optical Soc. Am.*, **38**, 226 (1948).
3. H. A. KLASENS, W. RAMSDEN, AND CHOW QUANTIE, *J. Optical Soc. Am.*, **38**, 60 (1948).
4. F. SEITZ, *Trans. Faraday Soc.*, **35**, 74 (1939).
5. N. F. MOTT AND R. W. GURNEY, "Electronic Processes in Ionic Crystals," Chapter VI, par. 3. Oxford University Press, Oxford (1948).
6. F. E. WILLIAMS AND H. EYRING, *J. Chem. Phys.*, **15**, 289 (1947).
7. F. URBACH, A. URBACH, AND M. SCHWARZ, *J. Optical Soc. Am.*, **37**, 112 (1947).
8. N. R. NAIL, D. PEARLMAN, AND F. URBACH, "Preparation and Characteristics of Luminescent Materials," p. 190, John Wiley & Sons, New York (1948).

SOME NEW COMPLEX SILICATE PHOSPHORS CONTAINING CALCIUM, MAGNESIUM, AND BERYLLIUM[1]

ARTHUR L. SMITH

Tube Department, Radio Corporation of America, Lancaster, Pennsylvania

ABSTRACT

The simple silicates of Group II metals have long been known as phosphor bases. The only complex silicate containing two metals of Group II on which detailed information has been published is that containing zinc and beryllium. This paper establishes that under certain conditions of preparation $CaO \cdot MgO \cdot 2SiO_2$:Ti (diopside) is an efficient blue-emitting silicate under cathode-ray excitation. When cerium^{III} is used as an activator in this material, a highly efficient phosphor emitting mainly in the ultraviolet region is obtained. Manganese activation gives rise to a material emitting in two bands, orange and red, but the cathodoluminescent efficiency is poor.

The compound $2CaO \cdot MgO \cdot 2SiO_2$ (akermanite) activated by cerium^{III} also emits in the ultraviolet region and is characterized by an extremely short decay time (about 10^{-6} seconds). The $3CaO \cdot MgO \cdot 2SiO_2$ compound (merwinite) is very similar, but is slightly less efficient. Neither of these two materials is effectively activated by titanium or manganese.

Another complex silicate of unusual properties is $CaO \cdot BeO \cdot SiO_2$:Mn (trimerite) which has a cathodoluminescent efficiency comparable to that of the zinc-beryllium silicates, with a long, moderately high-level phosphorescence.

INTRODUCTION

All the simple silicates of Group II metals have been studied as phosphor matrices. Double, or complex, silicates of this group have also been investigated, most notably those in the ZnO-BeO-SiO_2 system. Leverenz (1) has a number of generic patents on complex silicates in which substitution of Group IV members for silicon, as well as some substitutions among Group II members themselves, is disclosed. His work includes combinations of the oxides of zinc, beryllium, cadmium, and magnesium with those of silicon, titanium, zirconium, and germanium. Kroeger (2, 3) has recently mentioned that $CaO \cdot MgO \cdot 2SiO_2$:Ti is an acceptable blue-emitting silicate, but did not detail any specific properties or preparative conditions.

There are, however, a number of other complex compounds of oxides of Group II metals with silica which heretofore have received little or no attention as phosphor bases. Such complexes may be found in the literature of ceramics, mineralogy, and crystallography. Table I shows those compounds which first received major attention. Included in the table are the metals found to be activators in these bases; parentheses enclose the activators which gave phosphors of relatively low efficiency.

The major difficulty of the investigation was the uncertainty whether

[1]Manuscript received May 31, 1949. This paper prepared for delivery before the Philadelphia Meeting, May 4 to 7, 1949.

these compounds could be prepared at temperatures attainable with the conventional phosphor-firing equipment. Previous work on the synthesis of these compounds had been in the region of 1350–1600 C. C. Burton Clark (4) has prepared all the compounds possible in the $CaO–MgO–SiO_2$ system and published complete x-ray diffraction information. The first concern was, therefore, whether compound formation could occur between 1150–1250 C, and, if it did, whether reaction would be complete within a reasonable time. It was subsequently determined that all of the compounds listed in Table I could be prepared in a pure form below 1250 C, provided suitable firing techniques were employed. Reactions were generally complete within 2 hours. During the investigation of the $CaO–MgO–SiO_2$ system, a definite reaction mechanism was discernible. The results of this phase of the problem will be published in the future in another journal.

MATERIALS

The purest grade of commercially available materials was used. The calcium carbonate, magnesium carbonate, silicic acid, and titanium dioxide

TABLE I. *Complex silicate phosphors*

Compound	Activator
$CaO·MgO·SiO_2$ (monticellite)	(Mn)
$CaO·MgO·2SiO_2$ (diopside)	Ce, Ti, (Mn)
$2CaO·MgO·2SiO_2$ (akermanite)	Ce
$3CaO·MgO·2SiO_2$ (merwinite)	Ce
$2CaO·ZnO·2SiO_2$ (hardystonite)	Ce
$CaO·BeO·SiO_2$ (trimerite)	Mn

were Mallinckrodt's Special Luminescent Grade. The zinc oxide, manganous carbonate, and beryllium oxide were chemically pure grade; the cerous nitrate was the best material available from Lindsay Light Company.

GENERAL PREPARATION OF PHOSPHORS

The treatment of all phosphors preparatory to firing was the same. The requisite quantities of materials were introduced into a pebble mill as a water slurry and milled from 8 to 24 hours. The milled slurry was dried at 120–180 C, and the resultant soft-caked product broken and placed in suitable silica-glass containers ready for firing.

Firing was conducted either in the hearth of the furnace under atmospheric conditions or in a tube in which a definite atmosphere, generally hydrogen plus steam, could be maintained. Fig. 1 shows the method of tube firing employed. The steam atmosphere was generated by permitting water from a reservoir to drip into the inclined tube. As the water ran down the tube it reached the heated portion and was rapidly vaporized. By this method, a steam atmosphere is maintained without the usual difficulties encountered when steam is piped into the system.

TESTING OF PHOSPHORS

Excitation conditions.—The materials were excited in the demountable chamber of the spectroradiometer previously described by A. E. Hardy

(5). The defocused electron beam had an accelerating potential of 8,000 volts and a current density of 0.5 microampere per square centimeter.

Emission characteristics.—The spectral distribution in the visible region was measured by means of the spectroradiometer. Emission in the ultraviolet region was determined with the aid of a Bausch and Lomb quartz monochromator. The two curves, obtained with the two instruments for a given material, were combined to give a single emission curve, such as those given in Fig. 4 and 5.

Efficiency of phosphors.—The peak and visual efficiency values of phosphors emitting in the visible region were obtained directly from spectroradiometer readings. Representative samples were used as arbitrary standards. The ultraviolet-efficiency values were determined by means of an unfiltered multiplier phototube having an S-4 surface. This ultraviolet-efficiency value (like the visual-efficiency value) differs from the peak-efficiency value in that in the ultraviolet measurement the total area under

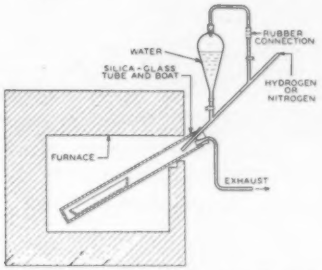

FIG. 1. Equipment used for phosphor firing

the emission curve is measured, while the peak efficiency is only the efficiency at the peak wavelength irrespective of the breadth of the emission curve.

Decay characteristics.—The absolute decay values of the cerium-activated compounds were determined by specialized equipment developed by O. H. Schade.[2] Relative measures of the persistence were obtained by a technique devised by A. E. Hardy. A metal baffle containing holes $\frac{1}{4}$ inch (.64 cm) in diameter was placed over the glass plate containing the puddled samples in such a way that each sample was exposed through one of the holes. The phosphors were then excited by single-line scanning at 15,750 cycles per second with an electron beam of 8 kilovolts and 8 microamperes per square centimeter. The emitted radiation fell on a multiplier phototube having an S-4 surface, and the signal from the phototube was fed into an oscilloscope. The pattern on the oscilloscope gave the build-up and decay as a function of time during the scan interval (Fig. 2). The retrace of the electron beam across the phosphor patch gave rise to a secondary pulse at about the middle of the decay interval. However, as can be seen in Fig. 2, this pulse is negligible.

[2]The equipment and associated circuits developed by O. H. Schade will be described in a paper to be published sometime in the future.

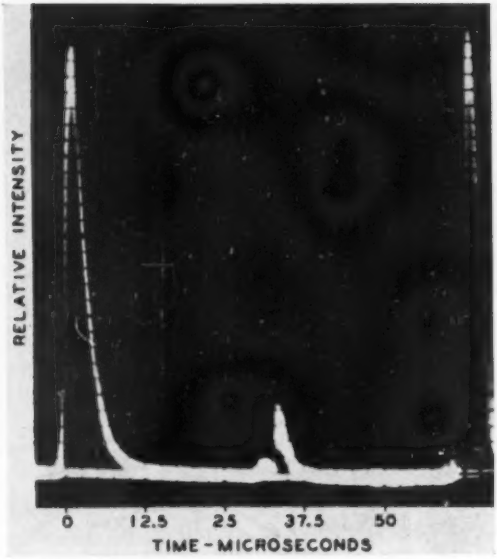

FIG. 2. Decay curve of $2CaO \cdot MgO \cdot 2SiO_2$:Ce

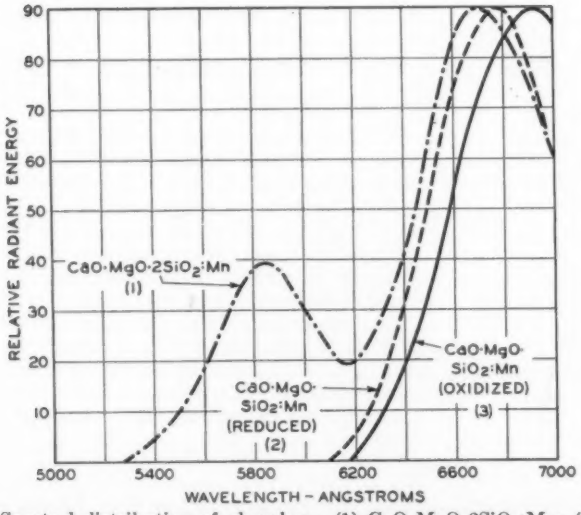

Fig. 3. Spectral distribution of phosphors. (1) $CaO \cdot MgO \cdot 2SiO_2$:Mn; (2) $CaO \cdot MgO \cdot SiO_2$:Mn (reduced); (3) $CaO \cdot MgO \cdot SiO_2$:Mn (oxidized).

The decay values of the $CaO \cdot BeO \cdot SiO_2$:Mn phosphor were found by utilizing square-wave pulsing of the electron beam. For these measurements also, a multiplier phototube and oscilloscope were employed in a system described by A. E. Hardy (5).

RESULTS

$CaO \cdot MgO \cdot SiO_2$ (Monticellite)

This material was the least efficient base material tested. Only manganese activation (concentration: 1–5 mole per cent) gave a measurable cathodoluminescence, and this value was but 5 per cent of the peak efficiency of manganese-activated willemite (Zn_2SiO_4:Mn). The emission was completely in the red region, as shown in Fig. 3. Different methods of preparation gave rise to some change in the spectral distribution. When hydrogen-

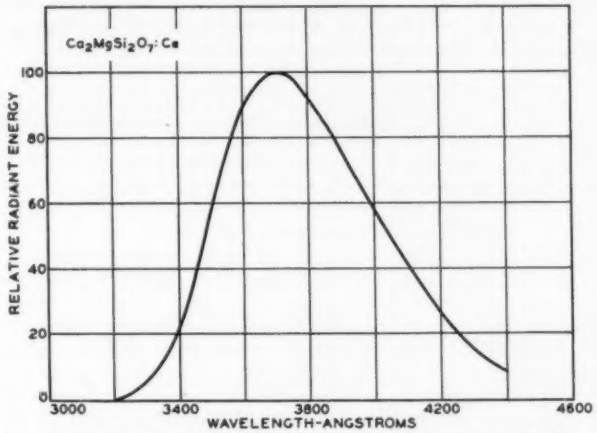

FIG. 4. Spectral distribution of phosphor $2CaO \cdot MgO \cdot 2SiO_2$:Ce

steam firing was employed, the emission was that indicated by curve 2 in Fig. 3. If, however, the carbonates were converted to nitrates by the addition of nitric acid, the mixture evaporated to expel all residual acid, and then fired in air at 1250 C, the emission was that of curve 3. Air firing of the carbonates with silica gave inhomogeneous products. Because the use of fluxing agents ($CaCl_2$ and/or $MgCl_2$) always gave rise to a product containing diopside ($CaO \cdot MgO \cdot 2SiO_2$), their use was discontinued.

Cerous activation (1–5 mole per cent) gave rise to some luminescence, but it was of such low order of magnitude that no accurate data could be obtained.

$2CaO \cdot MgO \cdot 2SiO_2$ (Akermanite)

Akermanite is not effectively activated by either titanium or manganese, but cerium^{III} activation gives rise to a phosphor of good efficiency. The emission lies mainly in the ultraviolet region, with the peak wavelength occurring at 3700 Å (Fig. 4).

The cerium-activated akermanite is best prepared by firing the requisite proportions of ingredients at 1250 C in a steam-hydrogen atmosphere. Without steam the reaction is incomplete in two hours, and the same type of gray product is obtained which Froelich found in cerium-activated phosphates (6). A less efficient phosphor resulted upon firing a material with Ce^{III} added as $CeCl_3$ in a nitrogen-steam atmosphere than upon firing the material with the cerium added as $Ce(NO_3)_3$ in a hydrogen-steam atmosphere.

The most noteworthy characteristic of this phosphor is its extremely short decay time, which is in the order of 10^{-6} seconds, being almost of the same order of magnitude as the ultraviolet decay component of zinc oxide phosphors (7, 8). Although a long time component is also present in this material, it is not objectionable for most tube applications.

When activated by manganese, inhomogeneous products were always obtained no matter what technique of firing was employed. This result is unusual because $2CaO \cdot MnO \cdot 2SiO_2$ is presumed to exist. This compound supposedly has the same basic structure as $2CaO \cdot MgO \cdot 2SiO_2$, and hence

TABLE II. *Efficiency and persistence of Ce^{III} activation (5 mole per cent) under cathode ray excitation (defocused beam, 8 kv, 0.5 μamp)*

Compound	Relative efficiency	Relative persistence
$CaO \cdot MgO \cdot 2SiO_2$	155	>>5
$2CaO \cdot MgO \cdot 2SiO_2$	120	2
$3CaO \cdot MgO \cdot 2SiO_2$	105	3
$2CaO \cdot ZnO \cdot 2SiO_2$	50	1

should form at least a limited solid solution. It may be concluded, therefore, that either $2CaO \cdot MnO \cdot 2SiO_2$ does not exist or it is not soluble in $2CaO \cdot MgO \cdot 2SiO_2$.

$3CaO \cdot MgO \cdot 2SiO_2$ (Merwinite)

Merwinite and akermanite are similar. Manganese and titanium bring about little or no emission when reaction is complete; incomplete reaction may be detected by a varicolored luminescence (orange plus red particles) with manganese as an activator.

When cerium activation is used, a phosphor is obtained which resembles akermanite in all respects, with the exception of slightly longer persistence and lower efficiency (Table II).

The preparation of this phosphor is the same as that of $2CaO \cdot MgO \cdot 2SiO_2$:Ce.

$CaO \cdot MgO \cdot 2SiO_2$ (Diopside)

This compound is activated by either titanium or cerium, and much less effectively by manganese. Although all the compounds in the CaO–MgO–SiO_2 system gave some emission when activated by titanium, this particular compound, when properly prepared, has peak efficiencies eight to ten times higher than the others. Titanium-activated willemite (Zn_2SiO_4:Ti) is the closest of any other silicate in peak value, being of the order of 70–75

per cent of diopside:Ti. The Zn_2SiO_4:Ti as a television screen material has the disadvantage of having a very narrow emission band (very much like the narrow band obtained with manganese). Diopside, however, has a much more desirable broad band. In comparison to other blue-emitting silicates. which have been either prepared or tested in this laboratory, the diopside:Ti is the most desirable in both efficiency and spectral distribution.

Titanium activation.—When this material is prepared by simply milling the requisite ingredients and firing, it is as inefficient as its congeners. X-ray diffraction examination of the products fired for two hours at 1250 C indicated rather poor crystal structure, even when steam was used. On the assumption that well-crystallized materials might provide more efficient phosphors, suitable fluxes were sought.

Chloride fluxes were chosen primarily because they could be washed from the final product. Calcium chloride proved quite effective in raising the efficiency; magnesium chloride less effective. A combination of the two, however, was more effective than either alone. When these chloride fluxes were used, it was noted that they reacted with the silica component, giving rise to volatile products containing both silicon and chlorine. The presence of these volatile products necessitated the use of excellent hood facilities for the furnace equipment. Because of these undesirable side reactions, compensation had to be made for the silicon volatilized and for the excess calcium and magnesium thereby introduced into the product.

Froelich (9) in his investigations of the simple silicates activated by titanium had found that the use of some sulfates as starting materials was beneficial. For this reason, the addition of sulfate to this compound was tested, the introduction being made through equimolar ratios of calcium and magnesium sulfates. These sulfates, too, acted as reactants, so further compensation for silica had to be made. When the proper ratios had been determined, the peak efficiency had been further raised so that an eight- to tenfold increase over that of the original mixture had been obtained.

The addition of the sulfate probably lowers the melting point of the mixed chloride flux in the same manner that Primak, *et al.* (10) had found in the sulfate-fluoride flux combination used in infrared-sensitive phophors. Whether lowering the melting point of the flux (and obtaining, therefore, better fluxing action) was responsible for the slightly increased efficiency, or whether it was due to the incorporation of sulfate ions as such, is not known. No lattice distortion could be found when the sulfate flux was used, but the amount incorporated could have been so small as to escape detection.

In addition to increasing greatly the peak efficiency, the flux also permitted some control over the particle size of the finished phosphor. After the remaining flux was washed free, the product was found to be of rather uniform particle size, very free flowing, and easy to handle.

The emission curve of $CaO \cdot MgO \cdot 2SiO_2$:0.05Ti is shown in Fig. 5. The very broad curve peaks at 4150 Å and is affected very little by either preparative conditions or titanium concentrations below 10 mole per cent. Although the peak efficiency is only 35 per cent that of manganese-activated zinc orthosilicate, it more efficiently converts electron energy into radiant energy because its emission in the short-wavelength region is so considerable. It is also to be noted that under cathode-ray excitation, diopside is the most efficient near-ultraviolet emitting material yet developed. Un-

fortunately, this high efficiency is obtained only under cathode-ray excitation; little or no emission is observed under 2537 Å excitation.

Cerium activation.—Diopside:Ce, when prepared in a manner similar to the preparation of akermanite:Ce, shows an emission curve of the same general type as given in Fig. 4, but with an over-all efficiency that is 25 per cent greater. The decay of this phosphor is at least two, and more probably three orders of magnitude slower than those previously described.

Manganese activation.—Although $CaO \cdot MgO \cdot 2SiO_2$:Mn is more efficient under cathode-ray excitation than other complex manganese activated calcium-magnesium silicates, its emission is of such low value that it is only of theoretical interest. Fluxes, hydrogen-steam firing, or other firing techniques do not appear to raise the efficiency to any great extent, nor change the emission as they did for monticellite.

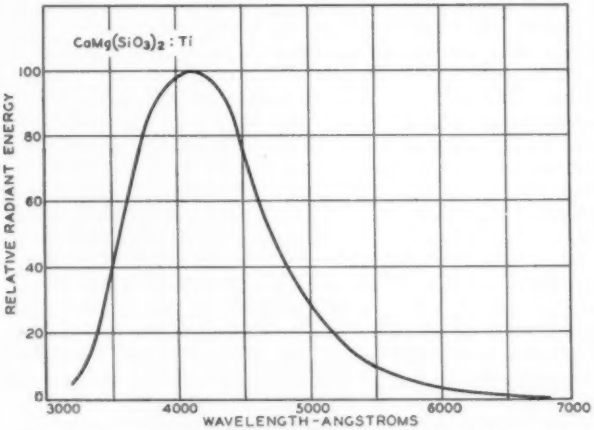

FIG. 5. Spectral distribution of phosphor $CaO \cdot MgO \cdot 2SiO_2$:Ti

As previously reported (11), the emission spectrum of this material exhibits two peaks (Fig. 3). Because the calcium ions in diopside are in eightfold coordination and the magnesium in six, the conclusion was drawn (11) that manganese in eightfold coordination exhibits yellow to orange emission. This is an extension of the coordination picture of Linwood and Weyl (12), and Schulman (13), the complete picture now showing green emission when manganese is in fourfold coordination, red emission in sixfold coordination, and yellow to orange emission for eightfold coordination. This hypothesis is still being subjected to further experimentation. It is significant that the heights of the two peaks are most affected by firing variations, with the red peak increasing at the expense of the orange as the firing time is increased. This condition cannot be attributed to incomplete reaction, because the x-ray diffraction photographs of materials showing both bands will show only the diopside structure. A more plausible explanation is that a diffusion process is operative in which manganese diffuses from the calcium lattice sites to those of magnesium with a corre-

sponding decrease in the orange emission and a corresponding increase in the red. Since this work is still incomplete, further discussion must await additional experimental evidence.

$2CaO \cdot ZnO \cdot 2SiO_2$ (Hardystonite)

$2CaO \cdot ZnO \cdot 2SiO_2$:Ce is prepared in the same way as its magnesium analogue with the exception that the firing temperature is 1000 C instead of 1250 C because fusion occurs at about 1100 C. In this preparation a plentiful supply of water vapor is essential to shift the equilibrium of the reaction

$$Zn + H_2O \rightleftharpoons H_2 + ZnO$$

far to the right.

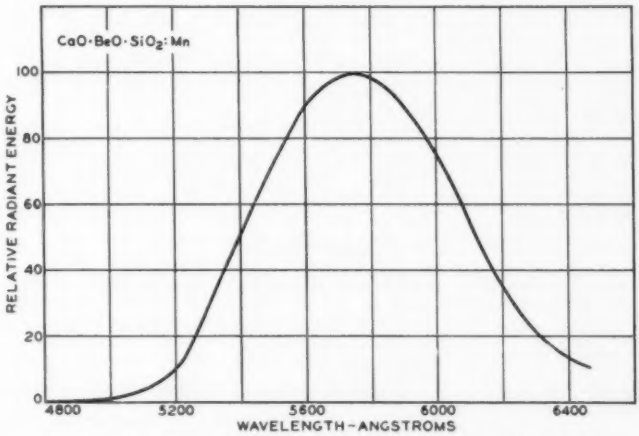

FIG. 6. Spectral distribution of phosphor $CaO \cdot BeO \cdot SiO_2$:Mn

Although the cathodoluminescent efficiency of the phosphor is less than half that of $2CaO \cdot MgO \cdot 2SiO_2$:Ce, its decay time is measurably shorter. Of all the cerium-activated materials tested, the decay time of this phosphor approaches most closely that of the ultraviolet band of the zinc oxide phosphor.

$CaO \cdot BeO \cdot SiO_2$ (Trimerite)

Efficient phosphors could not be obtained in this base when cerium or titanium were used as activators. With manganese, however, a phosphor was obtained which had at least 80 per cent of the cathodoluminescent efficiency of the zinc-beryllium silicates. The spectral distribution of the emission curve is shown in Fig. 6. Of considerable interest is the fact that this curve shows but one emission peak, which is invariant for a wide range in the Ca/Be ratio. Only when this ratio is very high or very low is the shape of the curve changed appreciably. Of greater importance is the

$(CaBe)O/SiO_2$ ratio. As this ratio is reduced from 2, the color shifts slightly toward the red, but even this shift (about 150 Å in going from a ratio of 2 to 1) does not approach that which can be attained by variations in the $ZnO \cdot BeO \cdot SiO_2$ system.

The phosphorescence caused by cathode-ray excitation is of high level and long duration (decays to 1 per cent of original value in 500 milliseconds). As yet this material does not compare with the cascade type screen or with the zinc-magnesium fluoride type, but it may find application where some intermediate phosphorescence of the e^{-t} type is desired.

CONCLUSION

Within the framework of this investigation, phosphors of very diverse properties have been discovered—$CaO \cdot BeO \cdot SiO_2$:Mn with an exceptionally high cathode-ray excited phosphorescence, and the cerium-activated silicates, $2CaO \cdot MgO \cdot 2SiO_2$:Ce, $3CaO \cdot MgO \cdot 2SiO_2$:Ce, and $2CaO \cdot ZnO \cdot 2SiO_2$:Ce with persistences so short that they approach that of the ultraviolet band of ZnO:(Zn).

In addition, a simple and practical method for the preparation of titanium-activated diopside ($CaO \cdot MgO \cdot 2SiO_2$) has been developed. This material is an efficient blue-emitting silicate.

Further work on the materials reported here is necessary and desirable, particularly to obtain more detailed and precise decay curves. Other combinations of Group II metal oxides with silica are already under investigation and give promise of phosphors of theoretical as well as practical interest.

ACKNOWLEDGMENTS

Thanks are due A. E. Hardy and associates for the spectroradiometer and decay measurements, and to A. D. Power of RCA Victor Division, Harrison, New Jersey, for x-ray analysis. Acknowledgment is also given to D. H. Wamsley for encouragement of this work.

Any discussion of this paper will appear in the discussion section of Volume 96 of the TRANSACTIONS of the Society.

REFERENCES

1. H. W. LEVERENZ, U. S. Pat. 2,118,091, May 24, 1936; 2,143,077, Jan. 10, 1939; 2,171,145, Aug. 29, 1939; 2,212,209, Aug. 20, 1940; 2,274,272, Feb. 24 1942; 2,306,270, Dec. 22, 1942; 2,306,271, Dec. 22, 1942; 2,402,760, June 25; 1946.
2. F. A. KROEGER, *Philips Tech. Rev.*, **9**, 215 (1947).
3. F. A. KROEGER, "Some Aspects of the Luminescence of Solids," Table XXI, Elsevier Publishing Co., New York (1948).
3a. Since this article has been submitted for publication, details of Kroeger's methods have been disclosed in U. S. Patent 2,473,960, June 21, 1949. His method entails coprecipitation of ingredients, and subsequent firing without flux.
4. C. BURTON CLARK, *J. Am. Ceram. Soc.*, **29**, 25 (1946).
5. A. E. HARDY, *Trans. Electrochem. Soc.*, **91**, 221 (1947).
6. H. C. FROELICH, *Trans. Electrochem Soc.*, **91**, 241-263 (1947).
7. R. SCHRADER AND H. W. LEVERENZ, *J. Optical Soc. Am.*, **37**, 939 (1947).
8. "Flying Spot Cathode-Ray Tube 5WP15", RCA Tube Dept. Bulletin, Commercial Engineering Dept., RCA Victor Division, Harrison, N. J.
9. H. C. FROELICH, U. S. Pat. 2,415,124, Feb. 4, 1947.
10. W. PRIMAK, R. K. OSTERHELD, AND R. WARD, *J. Am. Optical Soc.*, **69**, 1283 (1947).
11. A. L. SMITH, *Trans. Electrochem. Soc.*, **93**, 349 (1948).
12. S. H. LINWOOD AND W. A. WEYL, *J. Optical Soc. Am.*, **32**, 443 (1942).
13. J. H. SCHULMAN, *J. Applied Phys.*, **17**, 902 (1946); also "Preparation and Characteristics of Solid Luminescent Materials," p. 406, John Wiley & Sons, Inc. (1948).

LUMINESCENCE AND CONDUCTION IN SOLID SOLUTIONS OF CERIUM SULFIDE IN STRONTIUM SULFIDE[1,2]

EPHRAIM BANKS AND ROLAND WARD[3]

Polytechnic Institute of Brooklyn, Brooklyn, New York

Solid solutions of Ce_2S_3 in SrS were prepared by fluxing with LiF. X-ray precision lattice constant measurements show a solid solubility of 1 atom per cent for nitrogen-fired samples and 10 atom per cent for H_2S-fired samples. This difference in solubility is connected with the formation of Ce_2O_2S by reaction with traces of oxygen or moisture in the nitrogen. The existence of such a high solubility limit is explained on the basis of the formation of vacancies in the cation lattice (Schottky defects). Measurement of ionic conductivity confirms this. From the x-ray and conductivity data, it is concluded that Ce enters the SrS lattice in the trivalent state and in substitutional positions. The luminescent properties of both series of solid solutions show a shift with increasing cerium concentration. The emission peak of the N_2-fired series shifted from 4900 Å (in a sample with 0.5 atom per cent Ce) to 5100 Å (in samples with 2 per cent Ce or more). The emission peak of the H_2S-fired samples shifts from 5050 Å (at 1 per cent Ce to 5700 Å (at 10 per cent Ce). In this series, all samples with 3 per cent Ce or more are only fluorescent, while those with lower Ce content are phosphorescent. These shifts are explained on the basis of a lowering of the bottom of the conduction band with respect to the emitting levels, causing the shift toward longer emission wavelengths, and with respect to the shallow phosphorescent traps, causing the transition from phosphorescence to fluorescence.

INTRODUCTION

To acquire an understanding of the nature of the "active centers" in phosphors, it would appear to be most essential to know the valence state of the impurity ions and whether they enter into the base lattice in substitutional or interstitial positions.

In this laboratory, we were concerned with the infrared-stimulable phosphors of the type described by Urbach (1), Ward (2–4) and others. These are alkaline-earth sulfides and selenides activated with cerium and samarium or europium and samarium. Under the conditions of preparation, europium has been shown to be divalent (5) and samarium at least partially trivalent (6).

The present work was initiated with the object of obtaining information concerning the valence state of cerium in an alkaline-earth sulfide matrix. The method of approach was to examine the properties of the system at high cerium concentrations by means of x-ray diffraction and other applicable methods, and to deduce therefrom the situation in phosphors.

[1]Manuscript received June 13, 1949. This paper prepared for delivery before the Philadelphia Meeting, May 4 to 7, 1949. Part of the work reported here was performed under Contract NObsr-39045 with the Bureau of Ships.

[2]Abstracted in part from a dissertation presented by Ephraim Banks to the Graduate Faculty of the Polytechnic Institute of Brooklyn, in partial fulfillment of the requirements for the degree of Doctor of Philosophy.

[3]Present address: University of Connecticut, Storrs, Connecticut

EXPERIMENTAL

Samples were prepared by grinding together mixtures of strontium sulfide, cerium(III) sulfide, and lithium fluoride flux (6% by weight), in quantities calculated to give a definite atom per cent cerium, which is taken as the ratio of the number of cerium atoms to the total number of cerium and strontium atoms. These mixtures were heated for one hour at 1000 C, in atmospheres of purified nitrogen or hydrogen sulfide, after which they were allowed to cool in the furnace. The products were reground, a sample was taken for x-ray analysis, and the remainder was molded in a hydraulic

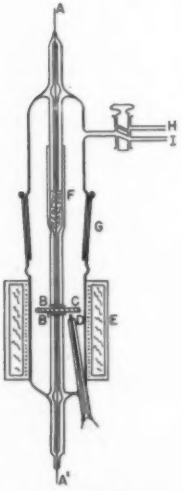

FIG. 1

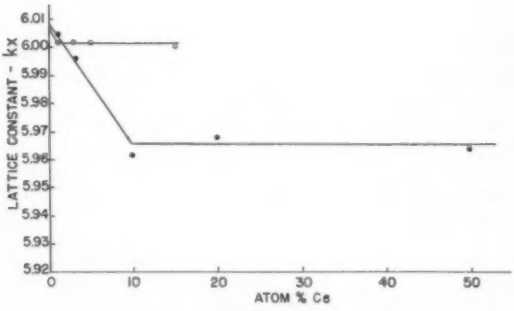

FIG. 2

FIG. 1. Sealed system for conductivity measurements. A, A′—leads to battery and galvanometer; B, B′—platinum contacts; C—sample; D—thermocouple; E—heater and insulation; F—spring assembly for maintaining contact pressure; G—ground glass joint; H, I—connections to vacuum pump and gas supply.

FIG. 2. Solubility of Ce^{+3} in SrS. Lattice constant *vs.* Ce concentration of Ce_2S_3-SrS mixtures. ○—fired in N_2, ● fired in H_2S.

press to give disks 3 mm thick. The disks were heated for one hour under the same conditions.

X-ray powder photographs were taken of the powders, and lattice constants were computed from the back-reflection lines, using the Straumanis technique to correct for film shrinkage. The disks were used for measurement of emission spectra and for conductivity measurements. Emission spectra were measured under constant ultraviolet excitation by means of a photomultiplier tube at the exit slit of a constant deviation spectrometer. Conductivities were measured as a function of temperature in the sealed apparatus of Fig. 1. The measurements were made by means of a battery and a sensitive galvanometer (5×10^{-10} amp/mm). Forward and reverse currents were measured alternately to minimize polarization effects.

RESULTS AND DISCUSSION

The results of x-ray analyses for two series of mixtures are shown in Fig. 2 in which the lattice constant is plotted against composition of the original mixture. The curve for the series of samples which were heated in nitrogen indicates a solubility limit at about one atom per cent Ce. The results obtained with the samples heated in hydrogen sulfide, on the other hand, show that much more extensive solution is obtained, the limit being at about 10 atom per cent cerium. The reason for this difference is not known, although it is probably due to the presence of some oxide introduced as moisture in the nitrogen. Cerous sulfide is rapidly converted to Ce_2O_2S when heated in moist nitrogen or hydrogen. The presence of hydrogen sulfide reverses this reaction. The decrease in lattice constant of the strontium sulfide which occurs on addition of cerium suggests that the cerium enters into substitutional positions and remains trivalent. The ionic radius of Ce^{+3} is 1.05 Å and that of Ce^{+2} is 1.13 Å, calculated according to Pauling (7). On the same basis, the radius of the divalent strontium ion is 1.13 Å. Thus, divalent cerium in substitutional solid solution in SrS should have very little effect on the unit cell dimensions. If either divalent or trivalent cerium ions entered into interstitial positions, an increase in lattice constant would be noted, rather than the observed decrease. Tetravalent cerium can be ruled out on the basis of the conditions of preparation.

For such a high solubility, it is reasonable to suppose that lattice defects are introduced to maintain electrical neutrality and because of the decrease in lattice constant, the occurrence of vacant cation positions is postulated. One hole (vacant Sr lattice point) should be introduced for every two cerium atoms in solid solution.

The presence of these holes should be detectable by their influence on the low-temperature ionic conductivity, as shown by Koch and Wagner (8).

The theory of ionic conductivity in solids is adequately treated in several places (9, 10). These treatments are based on the postulate that ionic conduction takes place through the migration of lattice defects under an electric field. The expression for conductivity takes the form:

$$\sigma = \sigma_0 e - (\tfrac{1}{2} W_0 + U_0)/kT$$

where σ = conductivity.
W_0 = energy required to form a pair of Schottky holes at absolute zero.
U_0 = activation energy for motion of an ion from one equivalent position to another.
k = Boltzmann constant.
T = absolute temperature.

The symbol σ_0 includes factors for the temperature dependence of the energies U and W and the vibrational frequency of the ions. By the introduction of permanent lattice defects due to the presence of trivalent cations we can, in effect, determine the energies U_0 and W_0 independently. At low temperatures the contribution of the thermally-formed holes to conductivity is negligible compared with the contribution from the permanent holes. The slope of the conductivity-temperature curves and the magnitude of the conductivity at low temperatures should be markedly dependent upon the cerium concentration. At high temperatures, the lattice defects intro-

duced thermally should make the major contribution to the conductivity, giving rise to curves which are essentially independent of the cerium concentration.

The conductivities of four of the samples prepared in hydrogen sulfide are shown in Fig. 3, which is a plot of log σ against $1/T$. At high temperatures, the curves fall approximately on the same straight line, as predicted by the theory. The average slope of the lines gives a value of about 24,000 calories per mole for $(\frac{1}{2} W_0 + U_0)$. At low temperatures, there is a change in slope which occurs at higher and higher temperatures as the cerium con-

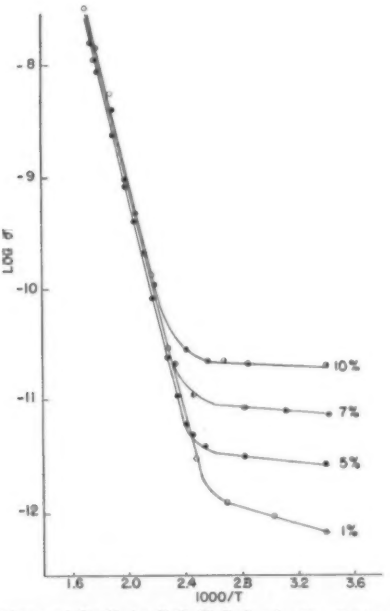

FIG. 3. Solid solutions of Ce_2S_3 in SrS–H_2S fired. ○—1 atom per cent Ce, ●—5 atom per cent Ce, ◐—7 atom per cent Ce, ◑—10 atom per cent Ce.

centration increases. This is to be expected, as the number of thermally-produced holes is a definite function of the temperature, and the slope begins to change as this number becomes comparable to the number of permanent defects. The behavior of the conductivity as a function of temperature confirms the conclusion that trivalent cerium goes into substitutional solid solution in strontium sulfide, with the formation of Schottky defects.

From the low-temperature slopes of the curves, values of U_0 were computed ranging from 1600 cal/mole for the one atom per cent sample to 250 cal/mole for the 10 per cent sample. By subtracting these values from the value of 24,000 cal/mole for $(\frac{1}{2} W_0 + U_0)$, we obtain values of W_0, the work required to form a pair of defects, ranging from 45,000 to 47,500 cal/mole. Such a value is considered reasonable for a divalent ion in a

rock-salt type lattice, when compared to the values of 23,000 cal/mole found for NaCl by Smekal (11) for sodium chloride and 25,000 cal/mole found for silver chloride by Koch and Wagner (8).

These solid solutions show an interesting variation in luminescent properties. The series of samples which were fired in nitrogen all showed green fluorescence and phosphorescence upon excitation with ultraviolet light. This emission appeared to be similar to the characteristic luminescence of cerium-activated strontium sulfide. The emission spectra of several of these samples are shown in Fig. 4. They show the expected decrease in brightness with increasing cerium concentration, since the optimum concentration for these phosphors is in the range of 100 to 250 ppm. The first peak in the emission shifts from about 4900 Å in the sample containing

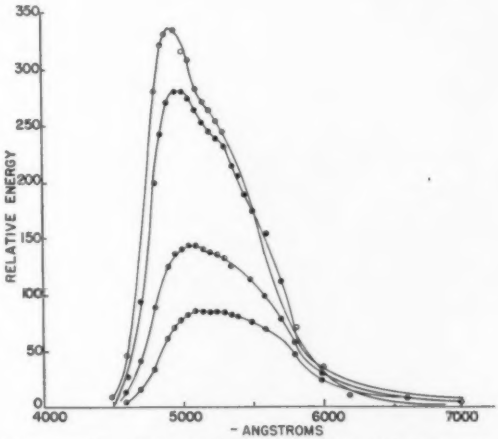

FIG. 4. Emission spectra, $SrS-Ce_2S_3-N_2$ fired. ○—0.5 atom per cent Ce, ●—1.0 atom per cent Ce, ◐—2.0 atom per cent Ce, ◑—3.0 atom per cent Ce.

0.5 per cent cerium to 5100 Å in the samples containing 2 to 3 per cent. This emission shift stops somewhere between one and two atom per cent Ce, with the peak remaining at a constant wavelength beyond this point.

The samples fired in hydrogen sulfide showed two marked differences from the nitrogen-fired samples. Among samples containing 1, 3, 5, 7, 10 20, and 50 atom per cent Ce, only the 1 per cent sample showed any persistent phosphorescence. In addition, there was a visible shift in emission color toward longer wavelengths as the cerium concentration was increased from green in the 1 per cent Ce sample to a deep red in the 10 per cent sample. The 20 per cent Ce sample showed a faint red fluorescence, while the 50 per cent sample was nonluminescent.

The emission spectra of these samples are shown in Fig 5. There is a shift in the first peak from 5050 Å at 1 per cent to 5700 Å at 10 per cent cerium, with a concomitant decrease in intensity.

This shift in spectral emission, paralleling a shift in lattice constant is common in phosphor systems where the lattice dimensions are changed by

the formation of solid solutions (e.g., SrS–CaS; ZnS–CdS). In this case, however, the change in lattice constant and the associated emission shift are achieved by the activator itself.

The change of emission from longer to shorter wavelengths is not consistent with the direction of change of the lattice constant. Thus, in the ZnS–CdS system, where the lattice constant is increased with increasing

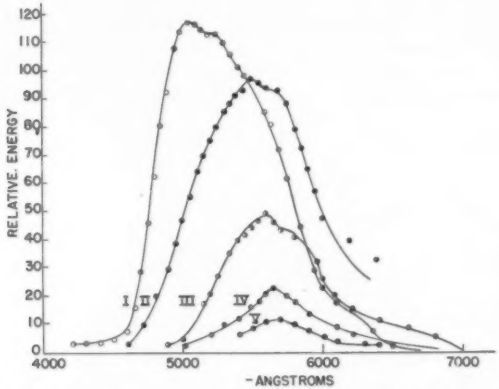

FIG. 5. Emission spectra, $SrS-Ce_2S_3$ solid solutions H_2S fired. ○I—SrS—1 mole per cent Ce, ●II—SrS—3 mole per cent Ce, ◑III—SrS—5 mole per cent Ce, ◐IV—SrS—7 mole per cent Ce, ◓V—SrS—10 mole per cent Ce.

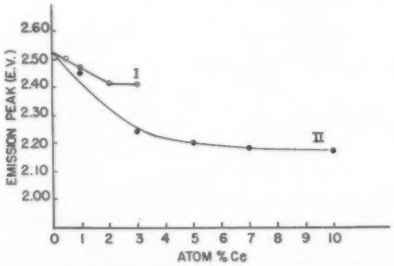

FIG. 6. $SrS-Ce_2S_3$ solid solutions, emission peak *vs.* Ce concentration. I—N_2 fired, II—H_2S fired.

CdS concentration, the emission shifts to longer wavelengths, while the incorporation of CaS in solid solution shifts the emission of SrS phosphors to longer wavelengths even though it causes a decrease in lattice constant. It appears that a fundamental explanation of these shifts will be quite complicated and that the lattice constant change is not very simply related to the emission shift.

A simple qualitative explanation based on the band theory of solids can be offered. In the solid solutions with which we are dealing, there seems to be a lowering of the bottom of the conduction band with respect to the

emitting levels as the concentration of cerium in solid solution is increased. By decreasing the energy separation between the conduction band and the emitting levels, we obtain a shift to longer wavelengths. This is illustrated in Fig. 6, showing peak emission (in electron volts) plotted against cerium concentration. The curves for both sets of samples show an energy decrease up to the solubility limit. In the curve for the nitrogen-fired samples, the shift stops between one and two atom per cent, while in the curve for the H_2S-fired samples, there is a continuous decrease up to 10 per cent.

The disappearance of phosphorescence between one and three per cent in the H_2S-fired samples is an indication that the conduction band is also being lowered with respect to the thermal traps responsible for normal phosphorescence. Their position, just as the emitting levels, appears to be fixed with respect to the shifting conduction band. Thus, as the conduction band is lowered, it begins to overlap the shallow traps, resulting in a disappearance of phosphorescence. Beyond the region of 1 to 2 per cent Ce, the shallow traps have all merged with the conduction band, and fluorescence only is observed, since the lifetime of an electron in the conduction band is of the order of 10^{-8} seconds. The persistence of phosphorescence in the nitrogen-fired samples is taken as an indication that the lowering of the conduction band has ceased before it could merge with all the shallow traps.

SUMMARY

1. By measurements of lattice constants and ionic conductivities of solid solutions of cerium(III) sulfide in strontium sulfide, it has been shown that cerium probably enters the strontium sulfide lattice in the trivalent state and in substitutional positions.

2. These solid solutions show a shift in emission peak toward longer wavelengths as the quantity of cerium in solid solution is increased. These shifts parallel a decrease in lattice constant, and are accompanied by a transition from phosphorescence to fluorescence. These phenomena are explained in terms of a lowering of the conduction band as the cerium concentration increases.

ACKNOWLEDGMENT

The authors are indebted to Professor I. Fankuchen of the Physics Department for his valuable advice on x-ray problems, and to Professor J. J. Dropkin for many helpful discussions on the theory and measurement of conductivity.

Any discussion of this paper will appear in the discussion section of Volume 96 of the TRANSACTIONS of the Society.

REFERENCES

1. F. URBACH, D. PEARLMAN, AND H. HEMMENDINGER, *J. Optical Soc. Am.*, **36**, 372 (1946).
2. W. PRIMAK, R. K. OSTERHELD, AND R. WARD, *J. Am. Chem. Soc.*, **69**, 1283 (1947).
3. A. L. SMITH, R. D. ROSENSTEIN, AND R. WARD, *J. Am. Chem Soc.* **69**, 1725 (1947).
4. "Preparation and Characteristics of Solid Luminescent Materials," John Wiley & Sons, Inc., New York (1948).
5. J. PRENER, Dissertation, Polytechnic Institute of Brooklyn, 1949.
6. G. COHEN, M.S. Thesis, Polytechnic Institute of Brooklyn, 1947.
7. L. PAULING, "The Nature of the Chemical Bond," p. 347, Cornell U. Press, Ithaca, N. Y. (1940)
8. E. KOCH AND C. WAGNER, *Z. physik. Chem.*, **38B**, 295 (1938).
9. N. F. MOTT AND R. W. GURNEY, "Electronic Processes in Ionic Crystals," Chapter II, Oxford U. Press, London (1940).
10. F. SEITZ, "Modern Theory of Solids," Chapter XV, sect. 132, McGraw-Hill Pub. Co., Inc., New York (1940).
11. A. SMEKAL, *Handbuch der Physik*, **24/2**, 881 (1933).

SOME SOLID SOLUTIONS OF THE RARE EARTH SULFIDES IN STRONTIUM SULFIDE[1]

HARRY L. YAKEL,[2] EPHRAIM BANKS, AND ROLAND WARD[3]
Polytechnic Institute of Brooklyn, Brooklyn, New York

ABSTRACT

The nature of various solutions of rare earth sulfides in strontium sulfide has been investigated. The procedure used depended essentially upon the precision determination of the lattice constants of the solutions.

La_2S_3, Ce_2S_3, Pr_2S_3, Nd_2S_3, Sm_2S_3, and Gd_2S_3 were prepared by heating the respective anhydrous chlorides in H_2S at elevated temperatures. Solutions of each were made up by intimately grinding weighed amounts of the rare earth sulfide, strontium sulfide, and a lithium fluoride flux and firing the mixtures for one hour in a stream of H_2S at a temperature of 1000 C.

The results of the lattice constant determinations on these solutions showed that all the rare earth sulfides studied are appreciably soluble in strontium sulfide. (The anomalously high solubilities of Nd_2S_3 and Sm_2S_3 cannot, at present, be explained.) The data also indicate that the rare earth ions in solution remain in the trivalent state. It was also shown that the solutions are substitutional in nature, two rare earth ions replacing three strontium ions in the SrS lattice. This substitution leads to the formation of holes in the cation lattice thus making the solutions defect structures.

INTRODUCTION

Lattice imperfections, or defects, in numerous crystalline substances have become the object of intensive investigation in recent years. This interest has resulted mainly from the fact that many properties of solids such as phosphorescence, electrical conductivity, and color centers can be explained, at least qualitatively, in terms of lattice defects.

In the investigation reported in this paper, the nature and extent of the solid solutions of several rare earth sulfides in strontium sulfide were determined. The procedure, which was suggested by previous investigations on infrared sensitive phosphors (1), depends upon the determination of the lattice constants of the solid solutions.

EXPERIMENTAL

Preparation of the rare earth sulfides.—The sulfides of trivalent lanthanum, cerium, praseodymium, neodymium, samarium, and gadolinium were prepared by heating the corresponding anhydrous chlorides in a stream of hydrogen sulfide at 700–800 C. The analyses of products given in Table I indicate that the products were reasonably pure.

[1]Manuscript received June 13, 1949. This paper, prepared for delivery before the Philadelphia Meeting, May 4 to 7, 1949, abstracted from a thesis by H. L. Yakel submitted to the Department of Chemistry of the Polytechnic Institute of Brooklyn, 1949, in partial fulfillment of the requirements for the degree of Bachelor of Science in Chemistry.

[2]Present address: California Institute of Technology, Pasadena, California.
[3]Present address: University of Connecticut, Storrs, Connecticut.

Preparation of the solid solutions.—Appropriate mixtures of each rare earth sulfide with strontium sulfide were prepared by grinding in an agate mortar. The composition of the mixtures is expressed as atom per cent rare earth ion in total cation content. A series of such mixtures was prepared for each rare earth sulfide, the number in each series depending on the solubility limit of the rare earth ion.

Approximately 12 per cent by weight of lithium fluoride was also ground into each mixture. This was done in order to facilitate the formation of the solid solutions upon heating the mixtures. It is highly improbable that the lithium fluoride served any other function (2).

The mixtures were placed in suitable platinum boats and heated in an atmosphere of hydrogen sulfide for one hour at 1000 C. The lattice constants of the products were then determined. The consistency of the results indicated that this heating period was sufficient to establish equilibrium. Additional experimental evidence of the attainment of equilibrium was obtained by approaching the equilibrium point in the opposite direction. The calculated amount of strontium sulfide was added to a 12 per cent solution of Gd_2S_3 to give a mixture containing 5 atom per cent of gadolinium. Upon heating this mixture, a product was obtained which gave the same lattice parameter as a 5 per cent solution prepared directly from Gd_2S_3 and SrS. This was done for several mixtures.

TABLE I

Compound	Color	% S found	% S theor.	% R.E. found	% R.E. theor.
La_2S_3	Yellow	24.9	25.7	75.2	74.3
Ce_2S_3	Violet	25.4	25.5	74.3	74.5
Pr_2S_3	Dark brown	25.4	25.4	74.5	74.6
Nd_2S_3	Dark brown	26.1	25.0	73.2	75.0
Sm_2S_3	Brown	24.6	24.2	75.3	75.8
Gd_2S_3	Brown	23.2	23.5	75.3	76.5
Yb_2S_3	Yellow	21.8	21.7	78.1	78.3

The presence of a hydrogen sulfide atmosphere during the firing procedure was very essential, as shown by the extreme difference in solubility between solutions fired in N_2 and those fired in H_2S (1).

X-ray techniques.—A Philips symmetrical back-reflection focusing camera was used for solutions containing relatively small amounts of rare earth sulfides. The Bradley and Jay extrapolation was used to obtain lattice constants to about one part in 10,000. With solutions containing higher percentages of rare earths, it was found that the back reflection lines became too broad and weak to give a satisfactory photograph with this camera. A Philips radian powder camera of conventional design was used, therefore, for these samples. The Straumanis technique was used to obtain the lattice constants, the Bradley and Jay extrapolation being again employed to obtain an accurate parameter. The average precision in these determinations was about one part in 5,000 although with some of the higher Sm and Nd samples the precision fell as low as one in 2,000.

The limits of solubility of the rare earth sulfides were taken as the percentage at which the lattice constants of the solutions became sensibly

constant. In most cases, this was checked roughly by observing the appearance of lines of a second phase in the Straumanis photographs of mixtures with higher rare earth ion content.

RESULTS

Limits of solubility.—The results of the lattice constant determinations for the Pr_2S_3–SrS series given in Table II are typical. It is evident from the lattice parameter data and from the appearance of the new phase in the forward reflections that the limit of solubility is 16.0 per cent.

Table III gives the results of similar solubility determinations for the other five rare earths studied. The lattice constant as a function of atom per cent rare earth ion for lanthanum, cerium, praseodymium, and gadolinium solutions are given in Fig. 1, while similar diagrams for neodymium

TABLE II. *Solutions of Pr^{3+} in SrS*

Atom % Pr	Lattice constant	Phases appearing in front reflections
0	6.0079	Pure SrS cubic
5	5.9858	SrS solid solution
10	5.9657	SrS solid solution
20	5.9410	SrS + additional phase lines
30	5.9395	SrS + additional phase lines with increased intensity

Solubility limit = 16 atom per cent

TABLE III. *Solubility limits for other rare earths*

Rare earth	Firing atmosphere	Solubility limit (atom % rare earth)
La^{3+}	H_2S	15.8
Ce^{3+}	H_2S	10.1
Pr^{3+}	H_2S	16.0
Nd^{3+}	H_2S	45.0
Sm^{3+}	H_2S	54.0
Sm^{3+}	N_2	4.5
Gd^{3+}	H_2S	11.6

and samarium appear in Fig. 2. It can be seen that the limits of solubility do not increase or decrease in any regular manner. At present no logical explanation of the unusually large solubilities of neodymium and samarium can be advanced.

It is interesting to note the marked difference in the solubility of samarium in SrS when the mixtures are heated in hydrogen sulfide and when they are treated in nitrogen. The data for the latter are given in Fig. 1. This is possibly due to the presence of oxygen or moisture in the nitrogen gas.

Nature of the solid solutions.—It has been established that, in the solid solutions of cerium in strontium sulfide, the cerium ions are trivalent and are in substitutional positions (1). The consequent creation of vacant cation sites causes the observed decrease in lattice constant. It is reasonable to suppose that the other rare earth ions with which we are concerned behave in a similar manner when dissolved in strontium sulfide, since in each case

the lattice constant decreases with the addition of rare earth ion. Additional evidence for this conclusion arises from the following considerations. The introduction of the same atomic percentage of any trivalent ion in substitutional solid solution should lead to the creation of a constant number

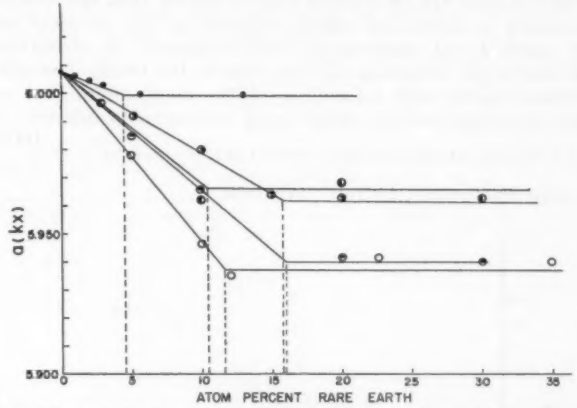

FIG. 1. Lattice constant *vs.* atom per cent rare earth for solid solutions of various rare earths in SrS. ◑—La^{+3} solutions, ◐—Ce^{+3} solutions, ◓—Pr^{+3} solutions, ●—Sm^{+3} solutions (N_2 fired), ○—Gd^{+3} solutions.

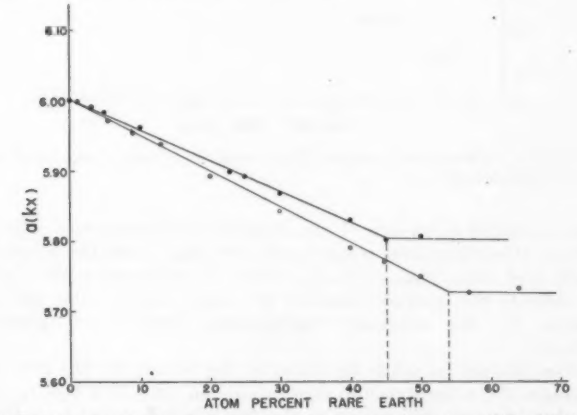

FIG. 2. Lattice constant *vs.* atom per cent rare earth for solid solutions of Sm^{+3} and Nd^{+3} in SrS. ○—Sm^{+3} solutions (H_2S fired), ●—Nd solutions (H_2S fired).

of vacant cation sites. The decrease in lattice constant caused by the presence of holes should, therefore, be the same for all equivalent solutions. Since the size of the rare earth ions decreases with increasing atomic number, however, we should expect that the lattice constant of equivalent solutions would decrease linearly with the radius of the rare earth cations.

In Fig. 3, the lattice constants of the 10 atomic per cent solutions of the rare earth ions are plotted against the ionic radii of the rare earths. The experimental points are, within experimental error, on a straight line, the slope of which is in the expected direction.

From these results the conclusion can be drawn that the samarium ion, in solid solution in strontium sulfide, remains in the trivalent state. The very high solubility of neodymium and samarium in strontium sulfide cannot be due to the reduction of these ions to the divalent condition.

The extraordinarily high solubilities of the neodymium and samarium ions in the strontium sulfide lattice is of considerable interest. The percentage of holes, y, introduced into the lattice is given by $y = \dfrac{100A}{A+2}$ where A is the atom fraction of the rare earth ion.

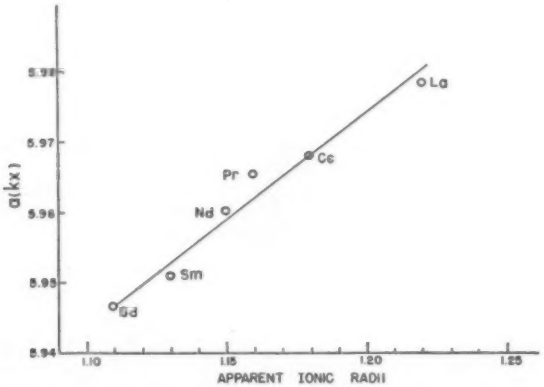

FIG. 3. Lattice constants of various 10 per cent solutions *vs.* apparent ionic radii as given by Goldschmidt.

For the saturated solutions of neodymium and samarium which are at 0.45 and 0.54 atom fractions respectively, we may write the formulae $Sr_{1.79}Nd_{1.47}X_{0.74}S_4$ and $Sr_{1.45}Sm_{1.70}X_{0.85}S_4$, where X represents the holes. The formulae indicate the average number of vacant cation sites per unit cell. The formula for the saturated gadolinium solution is approximately $Sr_{2.1}Gd_{0.6}X_{0.3}S_4$.

Some effort should be made to discover the reason for the greater stabilizing influence of the neodymium and samarium ions. It is conceivable that it may be due to some differences in the binding forces between the sulfide ion and the rare earth ions.

SUMMARY

Various solid solutions of rare earth sulfides in strontium sulfide have been prepared and their lattice parameters determined.

The results show that all the rare earth ions studied are extensively

soluble in strontium sulfide. Neodymium and samarium have abnormally high solubilities. These solutions are probably of the substitutional type in which two rare earth atoms replace three strontium atoms leaving a vacant cation site.

From the dependence of lattice constant change upon the size of the rare earth ion, it can be concluded that samarium is in the trivalent state when in solid solution with strontium sulfide.

A formula for the unit cell representing the number of "holes" is suggested.

Any discussion of this paper will appear in the discussion section of Volume 96 of the TRANSACTIONS of the Society.

REFERENCES

1. E. BANKS AND R. WARD, This JOURNAL, p. 297.
2. W. PRIMAK, H. KAUFMAN, AND R. WARD, *J. Am. Chem. Soc.*, **70**, 2043 (1948).

THE EFFECT OF MINOR ALLOYING ELEMENTS ON THE RATE OF DISSOLUTION OF ALUMINUM IN BASES[1]

M. E. STRAUMANIS

University of Missouri, School of Mines and Metallurgy, Department of Metallurgy Rolla, Missouri

AND

N. BRAKŠS

Chemical Laboratory, University of Latvia, Riga, Latvia

ABSTRACT

The dissolution rate of aluminum in 0.5*N* bases, NaOH, $Ba(OH)_2$, and NH_4OH is increased by the addition of several minor alloying elements, especially by those of low hydrogen overvoltage, e.g., Pt, Fe, and Cu. These metals act as cathodes of the local elements. The rate of solution of aluminum is shown to be proportional to the log of the concentration in per cent by weight of the alloying element up to 5 per cent. The activity of local currents should cease at approximately 0.000016 to 0.000004 per cent (for Fe and Cu).

The effect of alloying elements with high hydrogen overvoltage is entirely different. Zn, Cd, and Pb slightly increase the rate of dissolution of aluminum. Bi does not influence the rate, and Sn and Sb retard the dissolution rate. No simple relations were found for these alloys nor in the case of Mg and Ca when alloyed with aluminum.

INTRODUCTION

The question of whether the dissolution of aluminum in bases is caused by the activity of the local elements is still unsolved. Some observers, e.g., Centnerszwer (1), working with metals of different purity, 99.95 to 99.0 per cent, found no differences between the reaction rates in NaOH and NH_4OH. In consequence, it was concluded that in the dissolution of aluminum in bases the local elements are ineffective; i.e., the process is not electrochemical. Schikorr (2) also could prove that the degree of purity of aluminum was of slight importance when dissolving in strong bases. Müller and Löw (4), working with high purity aluminum made by Gadeau (3), stated that the local elements retain their effect even in basic solutions. Independently, the authors of this paper show that the rate of solution of 99.998 per cent aluminum distinctly increases on addition of small amounts of Cu or Pt salts to the basic solution (5). The present paper reports the rates of solution and the relationship between these rates and the concentration of the minor element in aluminum. These data indicate that the rate of dissolution of aluminum in bases is a function of the activity of local elements present.

[1]Manuscript received May 27, 1949. This paper prepared for delivery before the Chicago Meeting, October 12 to 15, 1949.

EXPERIMENTAL PROCEDURE

In the preparation of alloys of aluminum with different minor elements, the purest metals were used: Al [99.998%, Gadeau (3)], Mg (99.99%, Gadeau), Pt, Fe, Cu, Zn, Cd, Sn, Sb, Pb, Bi, Ca (Kahlbaum or Merck); only Si was 99.5 per cent pure. The relatively low purity of the Si accounts for the fact that few experiments with Al-Si alloys were run.

The weighed metals were placed into a small Al_2O_3 crucible, diameter 12–13 mm, which fits into a device of refractory glass. An atmosphere of pure dry hydrogen was maintained and the bottom of the vessel was put into a furnace at a temperature such that the melting point of the aluminum was exceeded by approximately 100 C. The melt, under hydrogen, was stirred vigorously for 30 minutes with an Al_2O_3 rod and then cooled. Then plates 10 mm in diameter and 4 to 5 mm thick were cut from the samples. Unfortunately, these sample alloys frequently contained cavities which rendered them useless. Cavities on the inside of the plates may have escaped observation and may be responsible for irregularities encountered during the dissolution process. This may have been true when dissolution rates were high.

The experiments were carried out in three highest purity bases: NaOH, $Ba(OH)_2$, and NH_4OH; all three 0.5*N*. The preparation of the plates for these tests and of the apparatus used for the measurement of the dissolution rate has been described previously (6). The volumes of evolved hydrogen were corrected to standard conditions of temperature, pressure, and dryness. The rates of dissolution were measured by these volumes which were expressed in mm^3/cm^2 min of dissolving aluminum surface by the relation:

$$V = \frac{\Delta v}{\Delta t F}.$$

The stirring speed was about 120 ± 5 revolutions per minute. The rates of the first five-hour periods, excluding the first 30 to 60 minutes which were erratic, were chosen for comparison. When the rate of dissolution was low, the tests were continued for longer times.

EXPERIMENTAL RESULTS

The minor alloying elements may be divided into three classes depending upon the effect of the element on the dissolution rate of aluminum in bases. The classes are as follows: (*a*) those elements that accelerate the dissolution of aluminum very effectively; (*b*) those elements which do not affect the rate appreciably; and (*c*) those elements which decrease the rate of solution.

The rates of dissolution of Al-Pt, Al-Fe, and Al-Cu alloys in NaOH, $Ba(OH)_2$, and NH_4OH.—These particular alloying metals, Pt, Fe, and Cu, were chosen for the following reasons: Pt, because it manifests the lowest hydrogen overvoltage; Fe and Cu, because they occur in perceptible quantities even in the purest aluminum and because of their low overvoltage. Table I indicates the progress of a dissolution experiment with time for an aluminum alloy containing 0.01 per cent Pt (by weight).

The tests start at a rapid rate as in all dissolution experiments with Al in bases (7). The rate decreases within an hour and then reaches a very flat maximum.

TABLE I. *The rate of dissolution of the Al-Pt (0.01%) alloy in 0.5N NaOH at 25 C.*

Time min	Experiment 13a		Experiment 13b	
	v_0 cm³	$\frac{\Delta v}{\Delta t}\,10^3$	v_0 cm³	$\frac{\Delta v}{\Delta t}\,10^3$
10	1.34	66.7	1.15	57.2
20	2.31	48.3	2.21	48.3
30	3.46	57.2	3.17	52.3
60	6.91	57.2	6.67	58.0
90	10.25	55.4	10.10	56.9
120	13.73	57.7	13.64	58.7
150	17.34	59.8	17.24	59.7
180	20.88	58.7	20.88	60.3
210	24.39	58.2	24.53	60.5
240	27.95	59.0	28.28	62.2
270	31.55	59.7	31.93	60.5
300	35.15	59.7	35.68	62.2
330	38.70	58.8	39.28	59.7
360	42.52	63.3	43.29	66.4
390	46.04	58.3	46.95	60.7
Averate rate 30-360 min.....		58.3		59.2

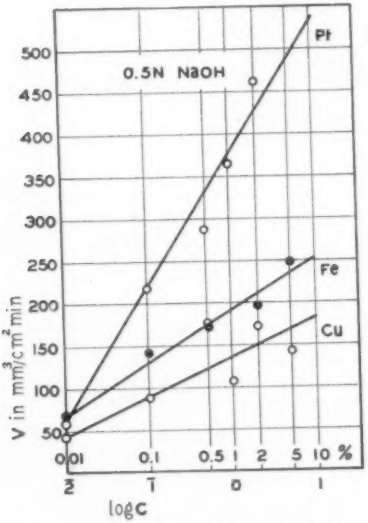

FIG. 1. The rate of solution of Al alloys in 0.5*N* NaOH is proportional to the log of concentration *C* in weight per cent of the nobler element (Pt, Fe, Cu).

In the figures and tables, average rates are given, which for the most part are the averages of two experiments, but in several cases are the averages of four or six tests. Fig. 1 shows the dissolution rate data obtained in 0.5*N* NaOH for the alloys containing Pt, Fe, and Cu.

The surface of the plates after the experiment was very uneven and covered with a thick layer of black precipitate, especially in the cases of higher percentage of alloying element. The increased surface may have induced a higher rate of solution while the precipitate may have retarded the reaction, since the diffusion of fresh alkali to the reaction surface was hampered. In many cases a flat maximum rate could be observed, but there were experiments which showed no maximum, but continued increasing rates. The average rates of the first 3 to 6 hours of reaction were chosen for comparison and a relationship between the rate of solution of the aluminum alloy and the concentration of the nobler alloying element could be represented by:

$$V = a + b \log C \qquad \text{(I)}$$

where V is the hydrogen evolution rate in mm^3/cm^2 min, C = per cent by weight, and b is the slope constant.

The agreement is much better if the rates obtained in the first 1 to 2 hours, after the $\frac{1}{2}$ hour of the initial period, were used for comparison when the reaction surface is more even. However, the authors believe that the choice described above is closer to the actual circumstances.

The three equations describing the rate of solution of Al-Pt, Al-Fe, and Al-Cu alloys in 0.5N NaOH are:

$$V_{\text{Al-Pt}} = 375 + 156 \log C \qquad \text{(II)}$$

$$V_{\text{Al-Fe}} = 193 + 63 \log C \qquad \text{(III)}$$

$$V_{\text{Al-Cu}} = 135 + 46 \log C \qquad \text{(IV)}$$

They are correct up to 5 per cent of the content of the nobler metal. The highest deviation (approximately 30%) from the equation could be observed only in one point for the case of copper [equation (IV), Fig. 1]. This deviation is one which frequently occurs in corrosion work.

A solution of 0.5N $Ba(OH)_2$ was chosen to determine the behavior of the above alloys in a strong divalent base.

The alloy containing platinum dissolved very irregularly so that the relationship of the rate of solution with the concentration of Pt in Fig. 2 is shown only as a broken line. The agreement with equation (I) was better in the case of Al-Fe and Al-Cu alloys. It is believed that this last alloy follows equation (I), although only two series of tests were made.

The equations representing the dissolution of Al-Fe and Al-Cu alloys in 0.5N $Ba(OH)_2$ are:

$$V_{\text{Al-Fe}} = 209 + 39 \log C \qquad \text{(V)}$$

$$V_{\text{Al-Cu}} = 130 + 24 \log C \qquad \text{(VI)}$$

The dissolution rates of Al-Pt and Al-Cu alloys in a weak base, 0.5N NH_4OH, were determined. The measured average rates of these alloys agree quite well (see Fig. 2) with the equations:

$$V_{\text{Al-Pt}} = 60 + 16 \log C \qquad \text{(VII)}$$

$$V_{\text{Al-Cu}} = 24 + 5 \log C \qquad \text{(VIII)}$$

The dissolution rates in NH_4OH show a more distinct tendency to gradually decrease than in other bases, since the $Al(OH)_3$ does not dissolve in

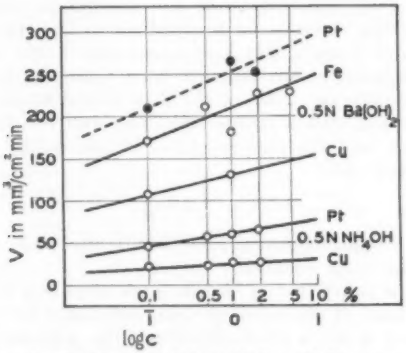

FIG. 2. The rate of solution of Al-Pt, Al-Cu, Al-Fe alloys in 0.5*N* $Ba(OH)_2$ and NH_4OH.

TABLE II. *The average rates of dissolution of Al with different minor elements in 0.5N NaOH, $Ba(OH)_2$, and NH_4OH at 25 C.*

Minor element in % by weight		Average rate *V* in mm³/cm² min		
		NaOH	$Ba(OH)_2$	NH_4OH
—	0	15.6	54	10.5
Zn	0.1	25	42	—
	0.5	60	—	—
	1.0	34	60	5
Cd	0.1	50	—	—
	0.5	22	61	—
	1.0	26	58	—
Sn	0.1	11	33	5-12
	0.5	10	40	8-30
	1.0	16	76	12-38
Sb	0.5	12	60	6
	1.0	14	32	7
	2.0	15	29	6
Pb	0.5	14	71	—
Bi	0.5	16	76	—
Si	0.5	47	46	—
Mg	0.1	16	68	3.1
	0.5	29	55	—
	1.0	41	63	2.7
	5.0	24	51	0.2
Ca	0.5	17	83	—
	1.0	20	52	—
	2.0	—	62	—

NH_4OH but partly coprecipitates with the metallic precipitate on the plates and hampers the diffusion of the fresh solution to a greater extent with other bases.

The rates of dissolution of Al alloys with other minor elements in 0.5N NaOH, $Ba(OH)_2$, and NH_4OH.—If the pure Al is alloyed with metals of high hydrogen overvoltage or with less noble elements than aluminum itself, e.g., Ca, Mg, entirely different velocity curves can be obtained. The average rates obtained with nine alloys are summarized in Table II and indicate that no simple relationship exists between the solution rate and the concentration of the specific alloying metal.

In the first row, the average rates of purest Al in 0.5*N* bases are mentioned for comparison (6), (8). From this table it can be seen that the velocity of dissolution of aluminum is:

(*a*) Slightly increased by: Zn, Cd, Mg, Si in NaOH
Cd, Mg, Pb, Bi, Ca in $Ba(OH)_2$
Sn in NH_4OH

(*b*) Not influenced by: Bi, Ca in NaOH
Zn, Si in $Ba(OH)_2$

(*c*) Retarded by: Sn, Sb, Pb in NaOH
Sn?, Sb in $Ba(OH)_2$
Sb, Zn, Mg in NH_4OH

The behavior of Si was not studied in detail because it contained Fe. The possibility exists that this element was the active part and not the Si itself.

DISCUSSION

The data show that even 0.01 per cent of a noble metal with low hydrogen overvoltage when alloyed with purest Al will accelerate the dissolution rate of the Al to a remarkable degree. Two questions arise: First, what will be the influence of these metals if present in Al in much smaller quantities? Second, do the small quantities of Fe and Cu which are still present in the Al influence its rate of solution? The calculated equations allow us to make some estimations in an attempt to answer these questions. From equations (III), (IV), (V), (VI), and (VIII), the amount of Cu and Fe present in the purest Al can be calculated using previous data for the dissolution rates of this metal in 0.5*N* NaOH, $Ba(OH)_2$, and NH_4OH (6), (8) 15.6, 54, and 10.5 mm^3/cm^2 min, respectively. For the Fe and Cu content of the plates dissolved, the following values were calculated:

	Per cent Fe in Al	Per cent Cu in Al
NaOH	0.0016	0.0026
$Ba(OH)_2$	0.0001	0.00068
NH_4OH	.....	0.002
analyses by Gadeau (3)	0.0002	0.0003

The order of magnitude in percentage of these minor elements in Al is the same as found by Gadeau by chemical analysis. A better agreement can scarcely be expected since the empirical equations are only approximate, e.g., changing the slope constant in equation (VIII) from 5 to 4, and this is quite possible, the Cu content is then calculated as 0.00013 per cent instead of 0.002 per cent, a result that is even below the result of Gadeau.

It is also possible that the distribution of minor elements throughout the Al ingot was not uniform, and the disks cut from the ingot could easily contain varying amounts of the minor element.

However, the calculations show that the aforementioned formulas reproduce correctly the relation between the velocity of dissolution of Al in bases and the content of minor elements (Fe and Cu) in the interval of 0.0002 per cent to 5 per cent or even to 10 per cent, that is, over a range of 4 or 5 powers of 10.

With regard to Pt, there is an exception. Since its activity is very violent, and it may be at low Pt concentrations in Al, the dependence is somewhat different from that shown by equation (II). Thus, the impurities present in the 99.998 per cent Al really influence its dissolution in bases and, finally, the purity of Al required in order not to dissolve at all in 0.5*N* bases at room temperature can be computed. For this condition equation (I) takes the form:

$$a + b \log C = 0$$

and values for C can be calculated as follows:

	Per cent Fe in Al	Per cent Cu in Al
NaOH	0.00087	0.0012
$Ba(OH)_2$	0.000005	0.000004
NH_4OH	.....	0.000016

The values for NaOH are evidently false, but the figures obtained dissolving Al in $Ba(OH)_2$ and NH_4OH show that the limit lies between 0.000004 and 0.000016 per cent by weight of Fe or Cu in Al. It is at present impossible to obtain a metal of such a high degree of purity. Of course, that is only a theoretical estimation because there will be some other factors that will not allow the velocity of dissolution of Al to approach zero in bases.

How the rate of dissolution of the alloys changes with concentrations other than 0.5*N* bases was not investigated.

CONCLUSIONS

The fact that the rate of dissolution of Al in bases increases gradually with the content of minor metals of low overpotential can be explained only by the activity of local elements. The noble metal particles act as cathodes, the Al as the anode. Further, the experiments show that the most active cathodes are the Pt particles. The Fe and Cu particles follow in that order. The sequence of metals with increasing hydrogen overpotential is exactly the same as shown by measurements both by us and by others (9). Finally, aluminum dissolving in bases shows the "difference effect," which was first described by Thiel and Eckell (10, 11) and recently shown by Streicher (12). The presence of the effect is a direct proof for the activity of local currents and, consequently, for the electrochemical theory of dissolution of aluminum.

Since metals with high overvoltage form local elements of low and very low current, they do not affect appreciably the dissolution rate of Al in

bases. For this reason the relation between velocity of dissolution and the concentration of minor elements in Al could not be detected previously and led, therefore, to the false conclusion of inertness of local elements in basic solutions. A semilogarithmic plot covering a wide range of concentration of the minor element in the Al allows one to find the equation in question. Other investigators, except Müller and Löw, did not have available Al of highest purity with which they could observe the effects of impurities over the full range of the curve. With the materials available to them, they were required to confine their studies to the middle section of the curve where the effect is scarcely observable.

Any discussion of this paper will appear in the discussion section of Volume 96 of the TRANSACTIONS of the Society.

REFERENCES

1. M. CENTNERSZWER, *Z. Elektrochem.*, **37**, 598 (1931).
2. G. SCHIKORR, *Z. Elektrochem*, **37**, 610 (1931); see also G. SCHIKORR," Die Zersetzungserscheinungen der Metalle," p. 76, J. A. Barth, Leipzig (1943).
3. R. GADEAU, Chimie & industrie **34**, 1021 (1934); *Metallwirtschaft*, **15**, 702 (1936).
4. W. J. MÜLLER AND E LÖW, *Aluminium*, **20**, 257 (1938).
5. M. STRAUMANIS AND N. BRAKŠS, *Korrosion u. Metallschutz*, **15**, 9 (1939).
6. M. E. STRAUMANIS AND N. BRAKŠS, *J. (and Trans.) Electrochem. Soc.*, **95**, 98 (1949).
7. U. R. EVANS, "An Introduction to Metallic Corrosion, p. 59," E. Arnold, London (1948).
8. M. E. STRAUMANIS AND N. BRAKŠS, *J. (and Trans.) Electrochem. Soc.*, **96**, 21 (1949).
9. G. SCHMID AND E. K. STOLL, *Z. Elektrochem.*, **47**, 360 (1941).
10. A. THIEL, *Z. Elektrochem.*, **33**, 370 (1927).
11. A. THIEL AND J. ECKELL, *Korrosion u. Metallschutz*, **4**, 121, 143 (1928).
12. M. A. STREICHER, *J. (and Trans.) Electrochem. Soc.*, **93**, 285 (1948).

THE VAPOR-PHASE DEPOSITION OF REFRACTORY MATERIALS[1]

I. General Conditions and Apparatus

I. E. Campbell, C. F. Powell, D. H. Nowicki, and B. W. Gonser

Battelle Memorial Institute, Columbus, Ohio

ABSTRACT

General conditions and apparatus for applying coatings of the refractory metals, carbides, nitrides, borides, silicides, and oxides by vapor-phase deposition are described. This process consists essentially of reducing, reacting, or decomposing a volatile compound of the coating material at a heated surface. Thick, adherent deposits have been obtained on a variety of bases, both metallic and nonmetallic. A few of the properties of the deposits are described, along with their limitations and potential uses as protective coatings for high-temperature service.

INTRODUCTION

Current interest in high-temperature processes has renewed interest in protective coatings for service at elevated temperatures. A cursory examination of tables of even the simplest refractory materials shows that conventional methods, such as electroplating, hot-dipping, painting, etc., are not suitable for application of coatings of many of these materials.

The most generally suitable processes for depositing or forming coatings of the refractory metals, carbides, borides, silicides, and nitrides are the vapor-deposition processes formerly used on a limited scale in preparing lamp filaments. In these processes, a volatile compound of the material which is to be deposited is passed over the work which is heated to a temperature at whch the compound is decomposed or reduced at the surface to form an adherent coating. The by-products of the plating reaction can either be pumped off, flushed off in a stream of "carrier" gas, or removed by combination with a mass of heated metal included in the system.

These processes should not be confused with the well-known "evaporation" and "sputtering" processes which are not considered here. The vapor-deposition processes can be used to deposit coatings of the most refractory materials at temperatures far below their melting points or at temperatures where their vapor pressures are negligible. Coatings varying from less than a micron to several millimeters in thickness can be formed in plating times varying from a few minutes to several hours in duration. Most vapor-deposition processes can be carried out either in a vacuum or at atmospheric pressure, and they always involve a chemical reaction at the plating zone.

Coatings made in this way at high temperatures are frequently more adherent and stable under high-temperature operation than materials deposited at low temperatures (as by electrodeposition), which have a greater tendency to flake away when heated.

[1]Manuscript received May 7, 1949. This paper prepared for delivery before the Philadelphia Meeting, May 4 to 7, 1949.

A considerable amount of information is available on specific coating processes, particularly on the formation of carbide coatings, and on the deposition of some of the refractory metals, but nearly all of the previous work has been confined to the coating of wires, and only a moderate amount of work has been directed toward the development of coating processes of general experimental and commercial utility.

In work at Battelle Memorial Institute for Project RAND on the analysis of methods for applying and/or forming refractory coatings, a comprehensive investigation of vapor deposition methods has been carried out. In the course of this work, procedures already outlined in the literature have been checked and missing data has been provided.

The present article is the first in a series of articles designed to provide a comprehensive summary of work at Battelle and elsewhere on the formation of refractory coatings by vapor-deposition methods and gives a general introduction to the vapor-deposition processes—including types of reactions used, coatings prepared, general conditions for formation of the various coatings, properties of the coatings, and possible applications of the coatings.

DISCUSSION

Coating materials

The selection of a coating material will normally be governed by five factors: (1) its melting point, (2) its resistance to attack by hot gases, (3) its mechanical properties at both low and high temperatures, (4) the cost of materials and labor involved in producing the coating, and (5) the strategic availability of the material. While a coating material can be conveniently evaluated from its properties in the order given, the use to which a coating is to be subjected will determine which factor is to be emphasized.

Table I lists the potentially useful refractory or high-melting materials which have been applied as coatings by vapor-deposition processes. These fall into six classes which are arranged as follows: (1) Metals, (2) Carbides, (3) Nitrides, (4) Borides, (5) Silicides, and (6) Oxides.

Exact formulas are not always given for compounds because of the frequent possibility of more than one being formed and existing together in solid solution.

Also listed in Table I are melting points and estimates of coating ductility and air-oxidation resistance—three properties of primary importance in evaluating coating materials.

Coating processes

Vapor deposition consists essentially of reducing or decomposing a volatile compound of the coating material upon the surface of a heated body. A summary of the conditions necessary for the practical employment of this method, as given by Van Arkel (1), an English version of which appears in Maxwell's report (2), follows: "The material must readily form a volatile compound which dissociates sufficiently at a temperature below the melting point of the coating material so that the partial pressure of the material in the vapor state is higher than the normal vapor pressure of the material at this temperature."

Two general plating methods are used: (1) Chemical reduction or reac-

TABLE I. *Vapor-deposited refractory coatings*

Deposit	Melting point, °C†	Ductility‡	Oxidation resistance*
(Metals)			
Tungsten	3410	2	4
Rhenium	3170	1	4-5
Tantalum	3000	1	5
Osmium	2700	3	5
Molybdenum	2620	2	5
Ruthenium	2500	3	4-5
Iridium	2454	2-3	4
Columbium	2415	1	5
Tantalum-columbium alloy	2300	1	5
Hafnium	1700-2230	1	3
Rhodium	1966	1	1
Chromium	1890	2	2-3
Zirconium	1860	1	3
Thorium	1830	1	3-4
Platinum	1773	1	1
Titanium	1725	1	3
Vanadium	1700	1	4
Uranium	1130	1	5
Tantalum-titanium alloy	—	1	3
Tantalum-zirconium alloy	—	3	4
Chromium-molybdenum alloy	—	—	4
(Carbides)			
Tantalum carbide + hafnium carbide (4 TaC + 1 HfC)	3940	3	3
Tantalum carbide + zirconium carbide (4 TaC + 1 ZrC)	3930	3	3
Hafnium carbide (HfC)	3885	3	3
Tantalum carbide (TaC)	3880	2-3	3
Carbon	3530	3	4
Zirconium carbide (ZrC)	3530	3	3
Columbium carbide (CbC)	3500	2-3	3
Titanium carbide (TiC)	3135	3	3
Tungsten carbide (WC)	d2865	3	5
Tungsten carbide (W_2C)	d2855	3	5
Vanadium carbide (VC)	2825	3	—
Molybdenum carbide (MoC)	d2690	3	5
Molybdenum carbide (Mo_2C)	d2685	3	5
Boron carbide (B_4C, B_6C)	2350-2500	3	3
Silicon carbide (SiC)	d1925	3	2
Chromium carbide (Cr_3C_2)	1890	3	—
(Nitrides)			
Tantalum nitride (TaN)	3085	3	5
Boron nitride (BN)	3000*	3	3
Hafnium nitride (HfN)	—	3	—
Zirconium nitride (ZrN)	2980	3	3
Titanium nitride (TiN)	2945	3	3
Vanadium nitride (VN)	d2050	3	—
Columbium nitride (CbN)	d2050	3	5
Tantalum carbide + tantalum nitride (TaC + TaN)	3305	2-3	3-5

TABLE I—*Continued*

Deposit	Melting point, C‡	Ductility§	Oxidation resistance¶
(Borides)			
Hafnium boride	3060	3	—
Zirconium boride	2990	3	2 3
Titanium boride	—	3	2-3
Tungsten boride	2920	3	3-4
Boron	2300	3	3
Tantalum boride	2000?	3	3
Molybdenum boride	2000?	3	3
Aluminum boride	—	3	3
Silicon boride	—	3	2-3
Vanadium boride	1300?	3	3-4
Chromium boride	—	3	1-2
(Silicides)			
Titanium silicide	2000?	3	4
Zirconium silicide	2000?	3	4
Molybdenum silicide	>1800	2	1
Tungsten silicide	—	—	1-2
Columbium silicide	—	2	4
Tantalum silicide	—	1-2	3
Chromium silicide	—	3	1-2
Silicon	1420	3	3
Chromium-molybdenum silicide	—	—	1-2
(Oxides)			
Zirconium oxide (ZrO_2)	2700	3	(1)†
Aluminum oxide (Al_2O_3)	2050	3	(1)†
Aluminum oxide + zirconium oxide ($Al_2O_3 + ZrO_2$)	2000	3	(1)†
Chromic oxide (Cr_2O_3)	1990	3	(1)†
Silicon dioxide (SiO_2) (glassy)	1713	3	1
Silicon dioxide (SiO_2) on aluminum oxide (Al_2O_3)	—	3	(1)†

d—Decomposes before melting.

* Under pressure.

† The coating was too porous to prevent oxidation of the base, although not oxidized itself.

‡ The melting points of the boride, silicide, and carbide coatings will, in practice, vary widely since the pure compounds are rarely obtained.

§ Ductility:

1. Capable of being severely drawn, rolled, or otherwise worked without failure.
2. Capable of withstanding slight deformation, or consisting of individually ductile crystals frailely bound together.
3. Incapable of being worked; of glass-like brittleness.

¶ Oxidation resistance:

Classed according to the temperature range in which the rate of attack by air would cause severe erosion or failure of the coated specimen within a few hours. 1. Above 1700 C; 2. 1400–1700 C; 3. 1100–1400 C; 4. 800–1100 C; and 5. 500–800 C. The oxidation rate also depends upon other factors, such as coat thickness and rate of air flow past the specimen, which have not been taken into account here.

tion at the surface. In this class are (*a*) hydrogen reduction of halides, (*b*) reaction of halides with a gas containing C, N, B, Si, or O, (*c*) displacement or reaction of the base material with one of the constituents of the gas phase. (2) Thermal decomposition at the surface: (*a*) at high temperatures

—halides and oxygen-containing compounds, and (*b*) at low temperatures —carbonyls and hydrides.

Most of these processes can be carried out in pyrex apparatus since the majority of the volatile compounds used develop the required vapor pressure below 550 C and the samples, themselves, can usually be heated internally. Where less volatile materials such as the halides of chromium and vanadium are used, however, quartz, vycor, or porcelain apparatus may be necessary.

Metal containers are satisfactory in some cases, but in other cases the corrosive nature of the reactants precludes the use of metal equipment, particularly in the plating zone.

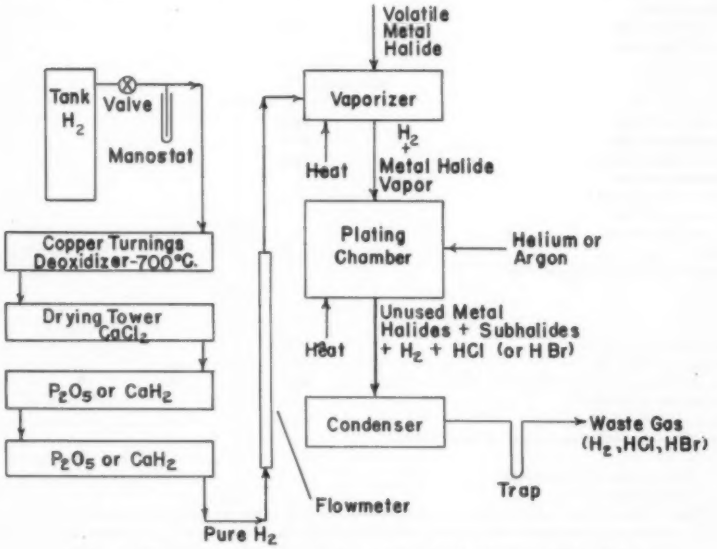

FIG. 1. Flow chart for vapor deposition by hydrogen reduction

The specimen is best heated by induced high-frequency currents, or by resistance heating, the form and composition of the specimen permitting. External furnace heating can be employed in some cases, but the plating efficiency is often low because of extensive deposition on the walls of the plating chamber.

A flow sheet for the hydrogen-reduction process is given in Fig. 1, and two sets of equipment for vapor-phase coating work are shown in Fig. 2 and 3.

The reactions and general conditions for depositing the refractory metals, carbides, nitrides, borides, silicides, and oxides are summarized in Table II. Rather than list all of the available reactions for depositing each material, the reaction considered best suited for that material by reason of convenience or quality of coating is given. Where no ideal coating method

exists, or where several reactions of equal value are available, more than one deposition reaction has been listed for a material.

In all of the plating processes except the halide decomposition method for Ti, Zr, Hf, Th, V, Cr, U, and Re [reaction 2 (*a*)], the plating atmosphere is usually prepared and mixed outside of and separately from the plating chamber. This requires large amounts of more-or-less pure auxiliary materials, such as hydrogen, halogens, hydrocarbons, nitrogen, carrier gases, etc., which are usually not conveniently recoverable after being used. With the halide decomposition process, a relatively small amount of halogen may in some cases be used to transport cyclically a large amount of metal between the low-temperature, halide-synthesis region and the high-temperature, metal-deposition point. As starting materials, one may use relatively impure crude metals or carbides. Those contaminants, chiefly, O, N, and

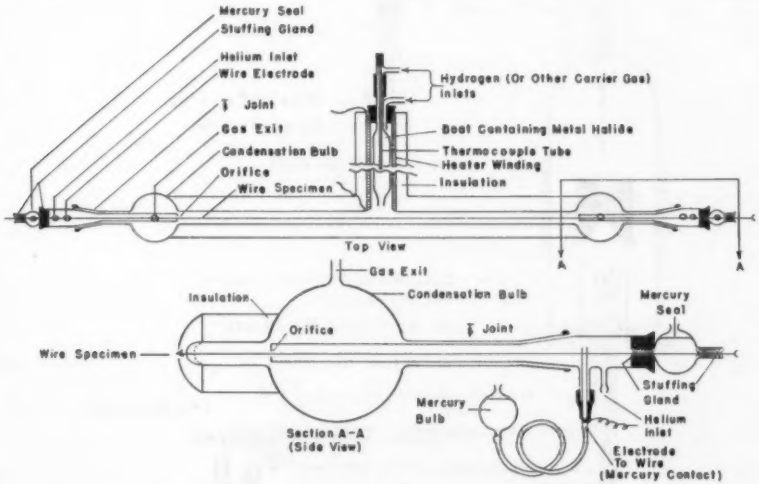

FIG. 2. Continuous flow, wire coating apparatus

C, which do not form volatile compounds are left behind and a purified metal is deposited. This process is not confined to depositing the metals listed, but can also be used with other metals which usually can be more conveniently deposited by other methods.

Coating characteristics

Physical properties.—The metals, with the exceptions of Os, Ru, and probably Ir, can be deposited in ductile form. They can be made hard and brittle, however, (and often inadvertently are) by the addition of traces of carbon, oxygen, nitrogen, or hydrogen compounds to the plating atmosphere. The carbides, nitrides, borides, silicides (except tantalum silicide and, to a certain extent, molybdenum silicide), oxides, boron, and silicon all deposit in an extremely hard, brittle form.

Effect of deposition temperature.—Of the several factors which influence

the nature of the deposit, the specimen temperature seems to be most important. Lower temperatures usually favor more finely crystalline deposits and high temperatures more coarsely crystalline deposits. Virtually amorphous deposits are obtained at the lowest deposition temperatures, and deposits of crystals several millimeters in diameter at the higher temperatures. At high temperatures, monocrystalline (or pseudomonocrystalline) deposits can be obtained if a monocrystalline base is used. At medium or low temperatures, the structure of the base has little or no effect upon the form of the deposit. The maximum deposition temperature in any case is gen-

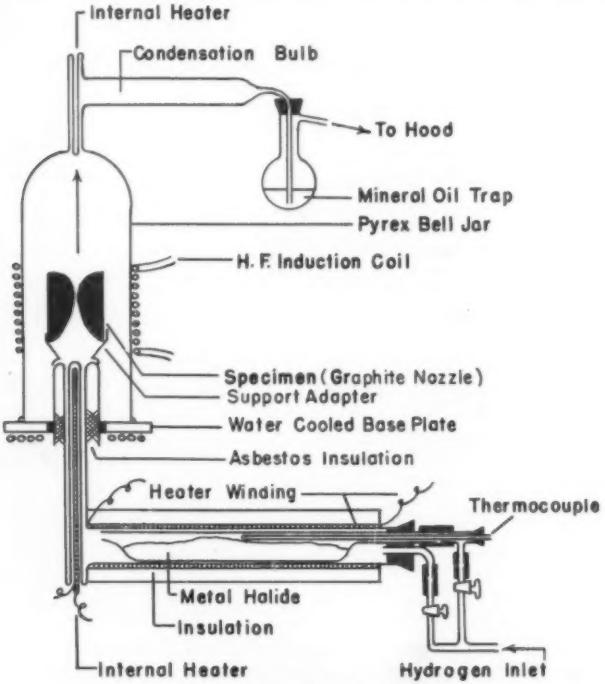

FIG. 3. Nozzle coating apparatus

erally the melting point of the base, of the coating, or of any reaction product or solid solution formed between the base and the coating.

The specimen temperature also affects the adhesion and cohesion of the deposit. The less stable plating compounds tend to be reduced or decomposed at a considerable distance from the heated surface at the higher temperatures. This causes nonadherent powder deposits, or the formation of nonvolatile decomposition products which are blown out of the plating zone before deposition can occur. The effect is especially noticeable in depositing Cb, Ta, Mo, and W by hydrogen reduction of the halides; SiO_2, Al_2O_3, ZrO_2, etc., by the CO_2+H_2 oxidation of the halides; and in the

TABLE II. *Vapor-deposition reactions*

Deposit	Reaction type‡	Deposition reaction	Deposition temp, C	Total gas pressure
		(Metals)		
Titanium	1(*a*)	$TiBr_4 + H_2 \rightarrow Ti + HBr$	900–1400	1 atm
Titanium	2(*a*)	$TiI_4 \xrightarrow{\Delta} Ti + I_2$	1200–1400	50 mm
Zirconium	1(*a*)	$ZrBr_4 + H_2 \rightarrow Zr + HBr$	900–1400	1 atm
Zirconium	2(*a*)	$ZrI_4 \xrightarrow{\Delta} Zr + I_2$	1300–1800	50 mm
Hafnium	2(*a*)	$HfI_4 \xrightarrow{\Delta} Hf + I_2$	1600	50 mm
Thorium	2(*a*)	$ThI_4 \xrightarrow{\Delta} Th + I_2$	1700	50 mm
Vanadium	2(*a*)	$VI_2 \xrightarrow{\Delta} V + I_2$	1100–1200	50 mm
Columbium	1(*a*)	$CbCl_5 + H_2 \rightarrow Cb + HCl$	600–1200	1 atm
Tantalum	1(*a*)	$TaCl_5 + H_2 \rightarrow Ta + HCl$	600–1400	1 atm
Chromium	1(*c*)	$CrCl_2 + M\,[+ H_2 + HCl] \rightarrow Cr + MCl_2$ (M = Fe, Ta, Mo, etc.)	900–1200	20 to 760 mm
Chromium	2(*a*)	$CrI_2, CrI_3[+ He] \xrightarrow{\Delta} Cr + I_2$	1000–1400	10^{-2} to 760 mm
Chromium	2(*b*)	$Cr(CO)_6 + H_2 \xrightarrow{\Delta} Cr + Cr_3C_2 + Cr_2O_3$	450–625	0.04 to 0.22 mm
Molybdenum	1(*a*)	$MoCl_5 + H_2 \rightarrow Mo + HCl$	500–1100	1 atm
Molybdenum	2(*b*)	$Mo(CO)_6 + H_2 \xrightarrow{\Delta} Mo + [C, H, O]$	450–750	<0.75 mm
Tungsten	1(*a*)	$WCl_6 + H_2 \rightarrow W + HCl$	500–1100	1 atm
Tungsten	2(*b*)	$W(CO)_6 + H_2 \xrightarrow{\Delta} W + [C, H, O]$	500–800?	<10 mm?
Uranium	2(*a*)	$UI_4 \xrightarrow{\Delta} U + I_2$	1600–1800?	50 mm
Rhenium	2(*a*)	$ReCl_3[+ N_2] \xrightarrow{\Delta} Re + Cl_2$	600–1800	1 atm
Ruthenium	2(*b*)	$Ru X_2 \cdot YCO \xrightarrow{\Delta} Ru + X_2 + CO$	600?	0.01–0.02 mm
Rhodium	2(*b*)	$Rh X_2 \cdot YCO \xrightarrow{\Delta} Rh + X_2 + CO$	600?	0.01–0.02 mm
Osmium	2(*b*)	$Os X_2 \cdot YCO \xrightarrow{\Delta} Os + X_2 + CO$	600?	0.01–0.02 mm
Iridium	2(*b*)	$Ir X_2 \cdot YCO \xrightarrow{\Delta} Ir + X_2 + CO$	600?	0.01–0.02 mm
Platinum	2(*b*)	$PtCl_2 \cdot 2CO \xrightarrow{\Delta} Pt + Cl_2 + CO$	600	0.01–0.02 mm
Tantalum-columbium alloy	1(*a*)	$TaCl_5 + CbCl_5 + H_2 \rightarrow Ta + Cb + HCl$	600–1200	1 atm
Tantalum-titanium alloy	1(*a*)	$TaBr_5 + TiBr_4 + H_2 \rightarrow Ta + Ti + HBr$	600–1200	1 atm
Tantalum-zirconium alloy	1(*a*)	$TaBr_5 + ZrBr_4 + H_2 \rightarrow Ta + Zr + HBr$	600–1200	1 atm
		(Carbides)		
Carbon	2(*a*)	$CCl_4 \xrightarrow{\Delta} C + Cl_2$	>1000?	50 mm
Boron carbide	1(*b*)	$BCl_3 + H_2 + CxHy^* \rightarrow B_4C + HCl[CH]$†	1200–2000	1 atm
Silicon carbide	1(*b*)	$SiCl_4 + H_2 + CxHy \rightarrow \alpha\,SiC + HCl + [CH]$	1300–2000	1 atm
Silicon carbide	1(*b*)	$SiCl_4 + H_2 + CxHy \rightarrow \beta\,SiC + HCl + [CH]$	2000–2400	1 atm
Titanium carbide	1(*b*)	$TiCl_4 + H_2 + CxHy \rightarrow TiC + HCl + [CH]$	1300–1700	1 atm
Zirconium carbide	1(*b*)	$ZrCl_4 + H_2 + CxHy \rightarrow ZrC + HCl + [CH]$	1700–2400	1 atm
Hafnium carbide	1(*b*)	$HfCl_4 + H_2 + CxHy \rightarrow HfC + HCl + [CH]$	2100–2500	1 atm
Vanadium carbide	1(*b*)	$VCl_4 + H_2 + CxHy \rightarrow VC + HCl + [CH]$	1500–2000	1 atm
Columbium carbide	1(*c*)	$Cb + H_2 + CxHy \rightarrow CbC + H_2 + [CH]$	1300	1 atm
Tantalum carbide	1(*c*)	$Ta + H_2 + CxHy \rightarrow TaC, Ta_2C, Ta_6C_5 + H_2 + [CH]$	1300–2900	1 atm
Chromium carbide	1(*c*)	$Cr + H_2 + CH_4 \rightarrow Cr_3C_2, Cr_7C_3 + H_2 + [CH]$	600–800	1 atm?
Molybdenum carbide	1(*c*)	$Mo + H_2 + CH_4 \rightarrow MoC + H_2 + [CH]$	700	1 atm?
Molybdenum carbide	1(*c*)	$Mo + H_2 + CH_4 \rightarrow Mo_2C + H_2 + [CH]$	800	1 atm?
Molybdenum carbide	2(*b*)	$Mo(CO)_6 + H_2 \xrightarrow{\Delta} Mo_2C + [C, H, O]$†	300–800	0.1–3 mm
Tungsten carbide	1(*c*)	$W + 3N_2 + 1H_2 + CxHy \rightarrow WC + H_2 + N_2 + [CH]$	1000–2200	1 atm
Tungsten carbide	1(*c*)	$W + H_2 + CxHy \rightarrow \alpha\,W_2C + H_2 + [CH]$	2100–2400	1 atm
Tungsten carbide	1(*c*)	$W + H_2 + CxHy \rightarrow \beta W_2C + H_2 + [CH]$	2440–2550	1 atm
Tungsten carbide	2(*b*)	$W(CO)_6 + H_2 \xrightarrow{\Delta} W_2C + [C, H, O]$	300–800?	<10 mm?

TABLE II—*Continued*

Deposit	Reaction type‡	Deposition reaction	Deposition temp, C	Total gas pressure
		(Nitrides)		
Boron nitride	1(*b*)	$BCl_3 + 3N_2 + 1H_2 \rightarrow BN + HCl$	1200–2000	1 atm
Titanium nitride	1(*b*)	$TiCl_4 + 3N_2 + 1H_2 \rightarrow TiN + HCl$	1100–1700	1 atm
Zirconium nitride	1(*b*)	$ZrCl_4 + 3N_2 + 1H_2 \rightarrow ZrN + HCl$	1100–2700	1 atm
Hafnium nitride	1(*b*)	$HfCl_4 + 3N_2 + 1H_2 \rightarrow HfN + HCl$	1100–2700	1 atm
Vanadium nitride	1(*b*)	$VCl_4 + 3N_2 + 1H_2 \rightarrow VN + HCl$	1100–1600	1 atm
Columbium nitride	1(*c*)	$Cb + N_2 \rightarrow CbN$	1000	1 atm
Tantalum nitride	1(*c*)	$Ta + N_2 \rightarrow TaN$	1000	1 atm
Tantalum carbide + tantalum nitride	1(*c*)	$Ta + N_2 + C_xH_y \rightarrow TaC + TaN$	1100–1200	1 atm
		(Borides)		
Boron	2(*b*)	$B_2H_6 \xrightarrow{\Delta} B + H_2$	400–600	1 atm?
Boron	1(*a*)	$BCl_3 + H_2 \rightarrow B + HCl$	800–1600	1 atm
Aluminum boride	1(*b*)	$AlCl_3 + BCl_3 + H_2 \rightarrow Al\ boride + HCl$	1000	1 atm
Silicon boride	1(*b*)	$SiCl_4 + BCl_3 + H_2 \rightarrow Si\ boride + HCl$	1100–1300	1 atm
Titanium boride	1(*b*)	$TiCl_4 + BCl_3 + H_2 \rightarrow Ti\ boride + HCl$	1000–1300	1 atm
Zirconium boride	1(*b*)	$ZrCl_4 + BCl_3 + H_2 \rightarrow Zr\ boride + HCl$	1700–2500	1 atm
Hafnium boride	1(*b*)	$HfCl_4 + BCl_3 + H_2 \rightarrow Hf\ boride + HCl$	1900–2700	1 atm
Vanadium boride	1(*b*)	$VCl_4 + BCl_3 + H_2 \rightarrow V\ boride + HCl$	900–1300	1 atm
Tantalum boride	1(*a*)	$Ta + BCl_3 + H_2 \rightarrow Ta\ boride + HCl$	1800–2000	1 atm
Chromium boride	1(*a*)	$Cr + BCl_3 + H_2 \rightarrow Cr\ boride + HCl$	1200–1600	1 atm
Molybdenum boride	1(*a*)	$Mo + BCl_3 + H_2 \rightarrow Mo\ boride + HCl$	1800–2000	1 atm
Tungsten boride	1(*a*)	$W + BCl_3 + H_2 \rightarrow W\ boride + HCl$	1800–2000	1 atm
		(Silicides)		
Silicon	1(*a*)	$SiCl_4 + H_2 \rightarrow Si + HCl$	900–1400	1 atm
Titanium silicide	1(*a*)	$Ti + SiCl_4 + H_2 \rightarrow Ti\ silicide + HCl$	1100–1500	1 atm
Zirconium silicide	1(*a*)	$Zr + SiCl_4 + H_2 \rightarrow Zr\ silicide + HCl$	1100–1500	1 atm
Columbium silicide	1(*a*)	$Cb + SiCl_4 + H_2 \rightarrow Cb\ silicide + HCl$	1100–1800	1 atm
Tantalum silicide	1(*a*)	$Ta + SiCl_4 + H_2 \rightarrow Ta\ silicide + HCl$	1100–1800	1 atm
Chromium silicide	1(*a*)	$Cr + SiCl_4 + H_2 \rightarrow Cr\ silicide + HCl$	1100–1400	1 atm
Molybdenum silicide	1(*a*)	$Mo + SiCl_4 + H_2 \rightarrow Mo\ silicides + HCl$	1100–1800	1 atm
Tungsten silicide	1(*a*)	$W + SiCl_4 + H_2 \rightarrow W\ silicide + HCl$	1100–1800	1atm
Chromium-molybdenum silicide	1(*a*)	$Cr\ on\ Mo + SiCl_4 + H_2 \rightarrow Cr\text{-}Mo\ silicide + HCl$	1100–1800	1 atm
While no specific reactions of the type $MCl_4 + SiCl_4 + H_2 \rightarrow MSi + HCl$ have been reported or carried out, the silicides should be readily prepared by this method.				
		(Oxides)		
Aluminum oxide	1(*b*)	$AlCl_3 + CO_2 + H_2 \rightarrow Al_2O_3 + CO + HCl$	800–1000	1 atm
Silicon dioxide	1(*b*)	$SiCl_4 + CO_2 + H_2 \rightarrow SiO_2 + CO + HCl$	800–1000	1 atm
Silicon dioxide	2(*a*)	$(C_2H_5)_4SiO_4 [+ H_2 \text{ or } He] \xrightarrow{\Delta} SiO_2 + [C, H, O]$	800–900	1 atm
Zirconium oxide	1(*b*)	$ZrCl_4 + CO_2 + H_2 \rightarrow ZrO_2 + CO + HCl$	800–1000	1 atm
Chromic oxide	2(*a*)	$[C_5H_7O_2]_3Cr + CO_2 \xrightarrow{\Delta} Cr_2O_3 + [C, H, O]$	1000	1 atm
Aluminum oxide + zirconium oxide	1(*b*)	$AlCl_3 + ZrCl_4 + CO_2 + H_2 \rightarrow Al_2O_3 + ZrO_2 + CO + HCl$	800–1000	1 atm

X = Cl, Br, or I; Y = 1, 1½, or 2.

* C_xH_y = methane, benzene, toluene, acetylene, naphthalene, carbon monoxide + hydrogen, etc.

† [CH], [C, H, O] = hydrocarbon decomposition products.

‡ Reaction type:

1. Chemical reaction:
   - (*a*) Reduction of halides.
   - (*b*) Reaction of halides with a gas containin C, N, B, Si, or O.
   - (*c*) Displacement or reaction of the base material with one of the constituents of the gas phase.
2. Thermal decomposition
   - (*a*) At high temperatures—halides and oxygen-containing compounds.
   - (*b*) At low temperatures—carbonyls and hydrides.

pyrolysis of carbonyl and carbonyl halide compounds (Cr, Mo, W, Ru, Rh, Os, Ir, Pt). The difficulty can be removed by lowering the specimen temperature or reducing the pressure of the plating atmosphere and thereby increasing the mean free path of the gas molecules.

Effect of coating-compound concentration.—The concentration (or pressure) of the reactants in the plating atmosphere affects the crystallinity of the deposits. The lower the pressure the more coarsely crystalline is the deposit. Thermal decomposition of compounds in vacuo usually results in deposits of readily visible crystals, while coatings made at atmospheric pressure are usually microcrystalline.

Effect of impurities.—Impurities such as oxygen, water vapor, or oxyhalides in the plating atmosphere may exert a pronounced effect in the form of the deposit as well as its properties. Difficulty in obtaining smooth deposits has frequently been traced to the presence of impurities such as oxygen or nitrogen which form nitrides or oxides in the deposit. The most pronounced effect of impurities is, however, the embrittlement of refractory metals such as tantalum, titanium, or vanadium by rather small quantities of oxygen, nitrogen, or carbon.

The purity of the deposit (as element or compound) depends upon the purity of the starting materials and upon the plating conditions. In the hydrogen-reduction process, the desired halide compound should be free of other volatile, reducible halides and of oxyhalides and halogens. The hydrogen used must be free of oxygen, nitrogen, and hydrocarbons if ductile metal deposits are desired. In depositing pure compounds, temperatures and reactant concentrations are so chosen, where possible, that the specimen temperature is above the melting point of the metal component of the coating, while the concentration of the nonmetallic component (C, N, B, etc.) is less than that of the metallic component as it exists in the desired compound. Thus, neither free metal nor free nonmetal can be deposited (3). This arrangement, however, does not prevent the formation of several mutually soluble compounds.

Rate of deposition

Deposition rates vary with the material deposited and the process used. Hydrogen reduction of certain metal halides proceeds at 7.5 to 65 microns per minute, but in some cases, particularly with the thermal decomposition processes, much lower deposition rates are obtained.

The thicknesses of vapor deposits may be varied within a wide range—from a few tenths of a micron to several millimeters. The average deposit runs from 25 to 250 microns in thickness, depending upon the type of service required of the coating.

Uniformity

Coating uniformity depends chiefly upon the uniformities of specimen temperature and of rate of supply of fresh plating atmosphere to all surfaces of the sample. Nonuniform specimen temperatures result in heavier deposits on the hotter portions, except under conditions where the higher temperatures produce premature reaction of the plating atmosphere. Uniform specimen temperatures are most readily obtained with external heating, but at the cost of lower plating efficiency. Internal heating, by

induction, will, in most cases, give uniform specimen temperatures if a judicious coil design has been employed.

A uniform supply rate of fresh plating atmosphere is more difficult to obtain than uniform specimen temperature, especially on stationary samples. With nonturbulent flow at near-atmospheric pressures, the material tends to deposit in pronounced streamlines and on the windward side of objects. Such nonuniformity can be reduced or eliminated by rotating or inverting the specimen during plating or between consecutive plating periods, and by proper baffling of the coating chamber so as to produce turbulent gas flow through it.

Operation at reduced pressure is sometimes useful in improving deposit uniformity, particularly in processes where premature reduction of the plating atmosphere presents a problem.

Another cause of nonuniform coatings is the "edge effect" whereby deposition occurs faster at sharp corners, edges, and highly curved surfaces. In most cases the excess material deposited at these points is not objectionable, but, if so, it can be easily removed by grinding or machining, or can be avoided by giving the specimen rounded edges and corners.

Efficiency of vapor-deposition reactions

Plating efficiency, as measured by the proportion of material deposited to material supplied as volatilized compound, varies greatly with the plating process and with the conditions used within any one process. The thermal-decomposition-in-vacuo processes are close to 100 per cent efficient. Values of 10 to 80 per cent have been observed in plating metals by hydrogen reduction of the halides, while the oxide-deposition processes are probably only a few hundredths or tenths of a per cent efficient, as normally conducted.

Products plated

A wide variety of products and materials have been coated by vapor deposition. Adherent, nonporous deposits of all of the materials listed in Table I have been obtained on one or more of the following: copper, nickel, iron, tantalum, molybdenum, tungsten, a variety of alloy steels, graphite, porcelain, quartz, alumina, pyrex, and carbide compounds. Metals have been coated on nonmetals and vice versa.

In addition to wire, rod, tubing, and strip, numerous articles such as pyrometer wells, die blocks, nozzles, crucibles, cyclotron- and x-ray-tube targets and magnetron rings have been coated. Most of the work has been carried out as a batch process, but certain of the refractory metals (Cb, Ta, Mo, W) have been coated on iron, copper, and molybdenum wires in diameters from 0.125 to 1.5 mm by a continuous-flow process.

The vapor-deposition processes have had only limited commercial application to date. A number of patents have been issued on the coating of wires for lamp filaments, but it is doubtful if any extensive commercial use has been made of filaments prepared in this fashion. The Foote Mineral Company is producing ductile zirconium in commercial quantities by the iodide decomposition process, and the similar production of ductile titanium is under development at the Battelle Memorial Institute and probably elsewhere.

The siliconizing of iron in a $SiCl_4$-H_2 atmosphere has been used to improve the corrosion resistance and chromizing by the pack method using $CrCl_2$ as the chromizing agent is finding increased use for the same purpose. Chromized iron was used by the Germans during the last war to extend the supply of scarce corrosion-resistant materials.

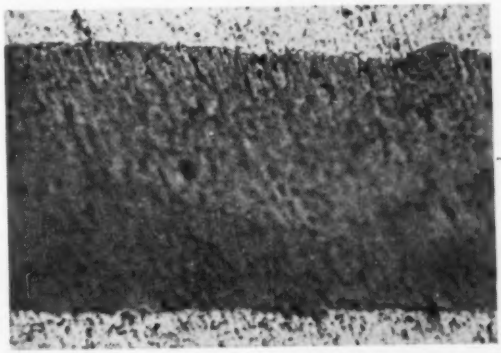

FIG. 4. Tantalum on 0.072 inch (1.83 cm) diameter O.F.H.C. copper wire, 15 minutes at 900 C, × 1000.

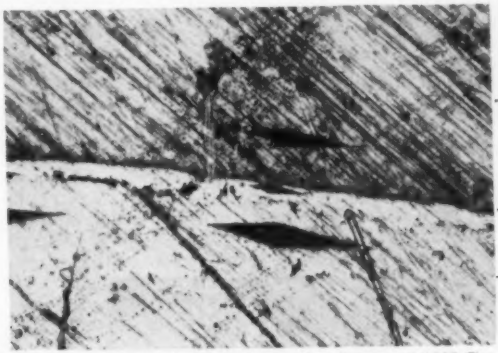

FIG. 5. Tantalum on high-purity iron, 30 minutes at 1000 C, × 250

The hydrogen-reduction process has been developed for depositing Cb, Ta, Mo, and W on commercially useful articles, but has not been exploited commercially as yet (4).

Micrographs of a number of typical deposits appear in Fig. 4 to 13.

Possible applications of vapor-deposition processes

1. In many applications, the body of an object is not excessively heated, yet fails through progressive attack initiated at some point in a thin skin at a heated surface. Vapor plating with a thin film of a high-melting ma-

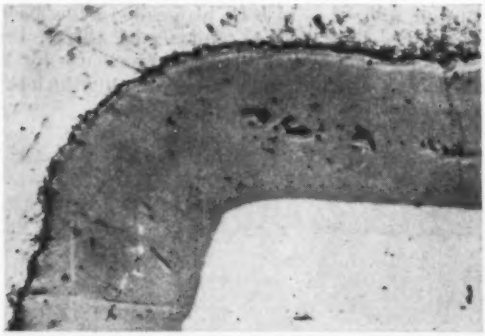

FIG. 6. Tantalum on nickel, 1300 C, × 750

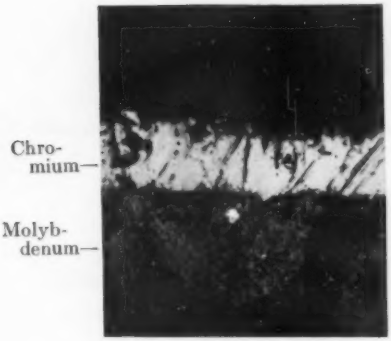

FIG. 7

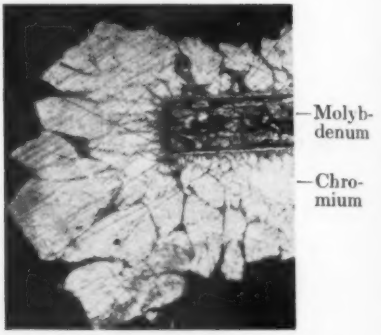

FIG. 8

FIG. 7. Chromized molybdenum (pack method). Six hours at 1000 C, × 500
FIG. 8. Chromium on molybdenum by the di-iodide decomposition-in-vacuo method. One hour at 1000 C.

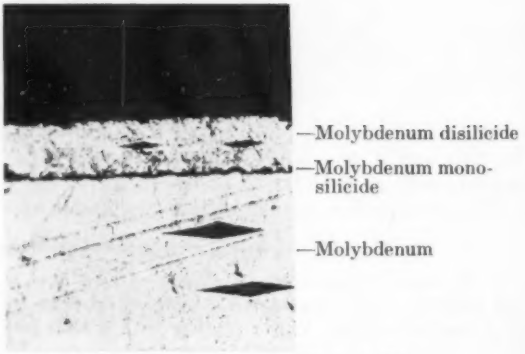

FIG. 9. Siliconized molybdenum. One hour at 1200 C, × 200

terial resistant to oxygen, nitrogen, water vapor, etc., would help to avoid this. Such materials exist in the carbides, nitrides, borides and some of the

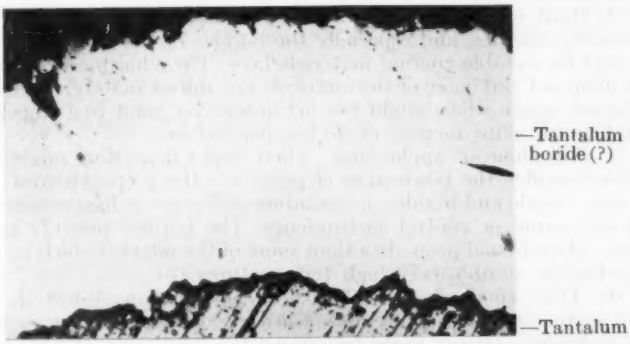

FIG. 10. Tantalum boride on tantalum, 15 minutes at 2000 C, × 500

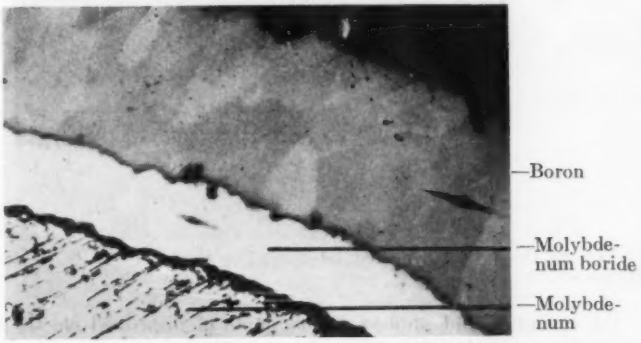

FIG. 11. Boron on molybdenum, 15 minutes at 1000 C, × 500

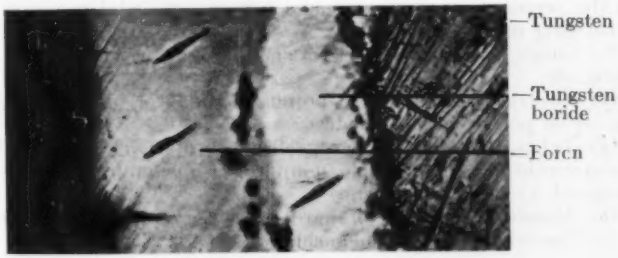

FIG. 12. Boron on tungsten, 15 minutes at 1500 C, × 500

silicides and oxides of the high-melting metals and the metalloids of the third, fourth, fifth, and sixth periodic groups. Specific applications might

be: (*a*) combustion chamber linings, (*b*) exhaust chamber linings, (*c*) turbine blade coatings, (*d*) valve linings, and (*e*) heat exchanger and regenerator elements.

2. Hard, erosion-resistant surfaces are required in some applications. The carbides, nitrides, and especially the borides of the aforementioned metals would be suitable coating materials here. Their hardnesses approach that of diamond, but some of the materials are, unfortunately, extremely brittle. Possible applications might be: (*a*) linings for solid fuel injection nozzles and shot-blasting nozzles, or (*b*) bearing surfaces.

3. Miscellaneous applications, where vapor deposition might expedite or make possible the fabrication of parts, are the preparation of:

(*a*) Nitride and boride superconductors for use in heat-sensitive elements of measuring or control instruments. The borides possibly possess even more phenomenal properties than some of the nitrides which become superconductive at unusually high temperatures (3).

(*b*) Thin, small elements for thermocouples, resistance thermometers, bolometers, etc. Elements more sensitive, of less time lag, or more stable at high temperatures could be prepared.

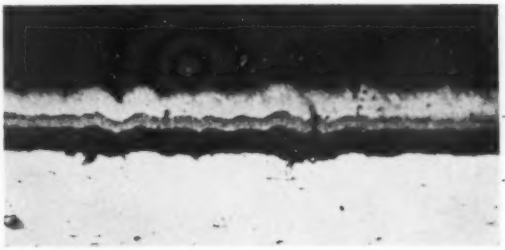

FIG. 13. $Al_2O_3+ZrO_2$ on molybdenum, two hours at 875 C, etched in boiling H_2O_2+HF. ×500.

(*c*) Vacuum- and photo-tube elements of improved electrical or optical properties (work function, secondary electron emission, spectral sensitivity).

(*d*) Transparent, aspheric lens elements prepared by a process similar to the preparation of paraboloidal mirrors by metal evaporation through a rotating mask.

(*e*) Large, transparent blocks or crystals of oxides such as SiO_2, ZrO_2, MgO, Al_2O_3, etc.

(*f*) Electrically conductive, porous coatings of high-melting, refractory metals on porous ceramic bodies.

(*g*) Tubes and sheets of hard, refractory materials (prepared by coating a removable core; for example, nonporous tungsten furnace tubes have been prepared by vapor deposition).

(*h*) Massive quantities of hard, refractory, or highly pure materials.

(*i*) Corrosion-resistant chemical ware.

CONCLUSIONS

Vapor-deposition processes can be used to deposit all of the refractory metals, carbides, borides, silicides, nitrides, and oxides. The deposition of

the metals and carbides and the formation of carbides, borides, silicides, and nitrides can be carried out under conditions that appear suitable for commercial development where conventional methods are either lacking or unsatisfactory. The deposition of oxides is considerably more difficult, as will be pointed out in a later article and, will, in all likelihood, be of value only in special applications, having little general utility.

The care of deposition and the necessity for careful control of plating and treating conditions vary considerably with the nature of the deposit desired and with the base material used, but the variety of reactions available for obtaining a given coating give the processes considerable flexibility and make it possible not only to obtain coatings of pure metals and compounds, but mixed coatings as well.

ACKNOWLEDGMENT

The authors gratefully extend their appreciation to the Rand Corporation and the United States Air Force for their permission to publish this paper which is based on a study supported by them.

Any discussion of this paper will appear in the discussion section of Volume 96 of the TRANSACTIONS of the Society.

REFERENCES

1. A. E. VAN ARKEL, "Reine Metalle," pp. 34-36, Julius Springer, Berlin (1939); Edwards Bros., Inc., Ann Arbor, Michigan (1943).
2. C. R. MAXWELL, "Hot Wire Reduction of Metals," PB Report No. 49564 (December 14, 1943).
3. C. AGTE AND K. MOERS, *Z. anorg. u. allgem. Chem.*, **198**, 233–75 (1931).
4. C. F. POWELL, I. E. CAMPBELL, AND B. W. GONSER, *J. (and Trans.) Electrochem. Soc.*, **93**, 258–56 (1948).